ORIGINAL PAPER

Isotopic evolution of prehistoric magma sources of Mt. Etna, Sicily: Insights from the Valle Del Bove

P. D. Kempton[1] · A. Spence[2] · H. Downes[2] · J. Blichert-Toft[3] · J. G. Bryce[4] · E. Hegner[5] · P. Z. Vroon[6]

Abstract

Mount Etna in NE Sicily occupies an unusual tectonic position in the convergence zone between the African and Eurasian plates, near the Quaternary subduction-related Aeolian arc and above the down-going Ionian oceanic slab. Magmatic evolution broadly involves a transition from an early tholeiitic phase (~ 500 ka) to the current alkaline phase. Most geochemical investigations have focussed on either historic (> 130-years old) or recent (< 130-years old) eruptions of Mt. Etna or on the ancient basal lavas (ca. 500 ka). In this study, we have analysed and modelled the petrogenesis of alkalic lavas from the southern wall of the Valle del Bove, which represent a time span of Mt. Etna's prehistoric magmatic activity from ~ 85 to ~ 4 ka. They exhibit geochemical variations that distinguish them as six separate lithostratigraphic and volcanic units. Isotopic data (^{143}Nd/^{144}Nd = 0.51283–0.51291; ^{87}Sr/^{86}Sr = 0.70332–0.70363; ^{176}Hf/^{177}Hf = 0.28288–0.28298; ^{206}Pb/^{204}Pb = 19.76–20.03) indicate changes in the magma source during the ~ 80 kyr of activity that do not follow the previously observed temporal trend. The oldest analysed Valle del Bove unit (Salifizio-1) erupted basaltic trachyandesites with variations in ^{143}Nd/^{144}Nd and ^{87}Sr/^{86}Sr ratios indicating a magma source remarkably similar to that of recent Etna eruptions, while four of the five subsequent units have isotopic compositions resembling those of historic Etna magmas. All five magma batches are considered to be derived from melting of a mixture of spinel lherzolite and pyroxenite (± garnet). In contrast, the sixth unit, the main Piano Provenzana formation (~ 42–30 ka), includes the most evolved trachyandesitic lavas (58–62 wt% SiO_2) and exhibits notably lower ^{176}Hf/^{177}Hf, ^{143}Nd/^{144}Nd, and ^{206}Pb/^{204}Pb ratios than the other prehistoric Valle del Bove units. This isotopic signature has not yet been observed in any other samples from Mt. Etna and we suggest that the parental melts of the trachyandesites were derived predominantly from ancient pyroxenite in the mantle source of Etna.

Keywords Prehistoric Etna · Sr:Nd:Pb:Hf isotopes · Mantle heterogeneity

Communicated by Dante Canil.

✉ P. D. Kempton
pkempton@ksu.edu

1 Department of Geology, Kansas State University, Manhattan, KS, USA

2 Department of Earth and Planetary Sciences, Birkbeck University of London, Malet Street, London WC1E 7HX, UK

3 Laboratoire de Géologie de Lyon, CNRS UMR 5276, Ecole Normale Supérieure de Lyon, Université de Lyon, 46 Allée d'Italie, 69007 Lyon, France

4 Department of Earth Sciences, University of New Hampshire, Durham, NH, USA

5 Department of Earth and Environmental Sciences and GeoBioCenter, Ludwig-Maximilians Universität, Munich, Germany

6 Department of Earth Sciences, Faculty of Science, Vrije Universiteit, Amsterdam, The Netherlands

Introduction

Mount Etna, Europe's largest active volcano, is located on the Mediterranean island of Sicily (Fig. 1) and lies in a complex tectonic setting near the convergence of the African and Eurasian plates. Eruptions of submarine and subaerial tholeiitic basalts between ~ 500 and 300 ka were gradually replaced by transitional to alkaline volcanism after ~ 250 ka via a succession of eruptive centres; this activity continues to the present day (McGuire 1982; Chester et al. 1985; Kieffer and Tanguy 1993; Scarth and Tanguy 2001; Patanè et al. 2006; Branca et al. 2008, 2011b). The magmatic evolution of Mt. Etna has been the subject of intense geochemical and isotopic research (e.g., Armienti et al. 1989; Marty et al. 1994; Tonarini et al. 1995, 2001; D'Orazio et al. 1997; Tanguy et al. 1997; Gasperini et al. 2002; Viccaro and Cristofolini 2008; Viccaro et al.
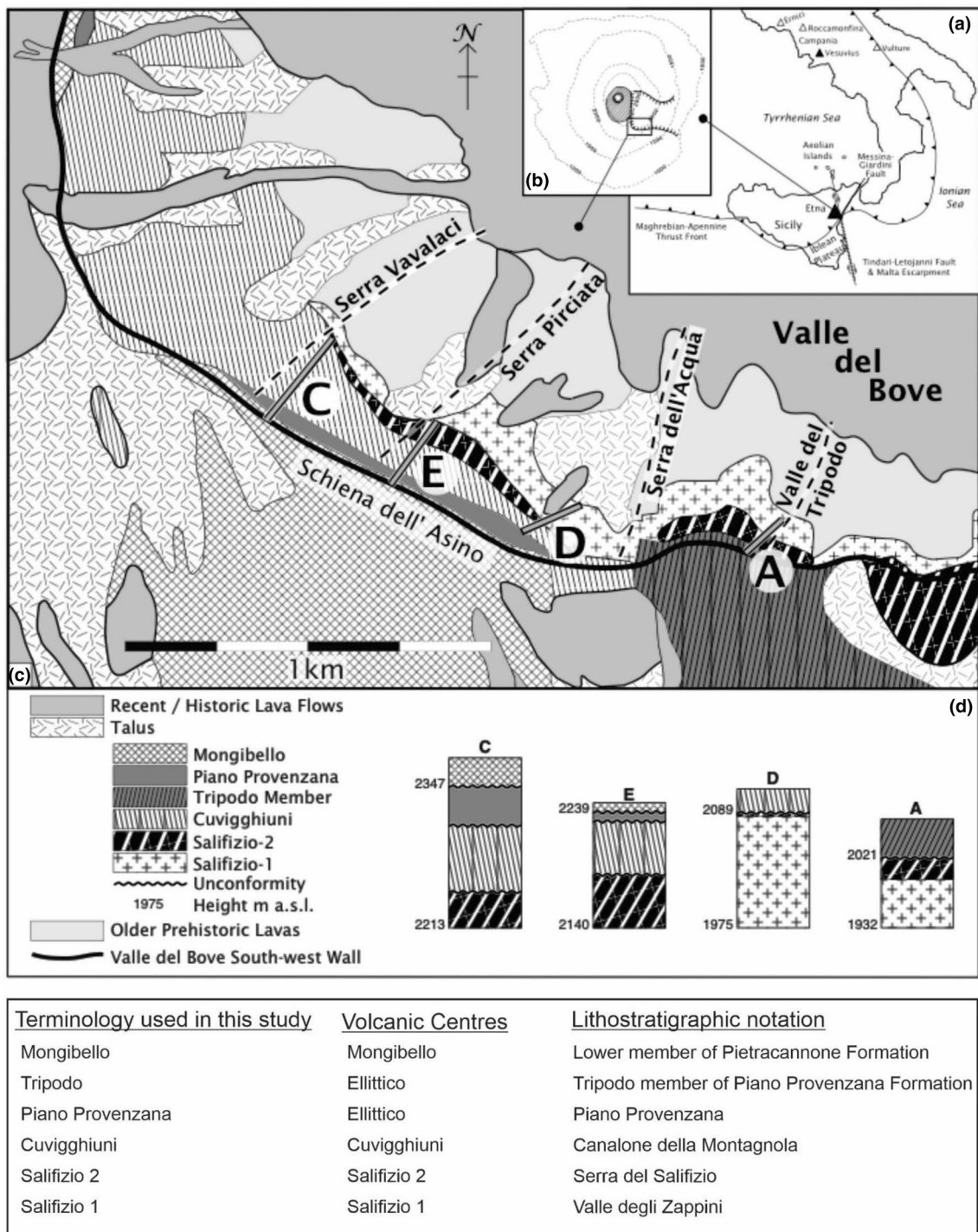
Fig. 1 **a** Public domain outline map of southern Italy with areas of interest indicated. **b** Outline of Mt. Etna with Valle del Bove, adapted from Chester et al. (1985). **c** Map of the southern wall of the Valle del Bove, adapted from the Geological Map of Etna Volcano (Branca et al. 2011b). Widths of sections A, D, E, and C are exaggerated for clarity. All samples analysed in this study were collected from one of the four sections labelled A, D, E and C. **d** Lithology of the six volcanic units as exposed in the four sections A, D, E and C

2011; Correale et al. 2014; Di Renzo et al. 2019), mainly using samples of recent (defined here as < 130 years old) and historic lavas, i.e., those erupted from the start of historic records to ca. 1890 CE. Sampling of prehistoric lavas

on Mt. Etna is generally hampered by the widespread cover of these younger (historic and recent) eruptive products. Note the age boundary between historic and prehistoric is undefined, due to lack of data; the youngest prehistoric

samples included here are < ~ 15-kyr old (D'Orazio et al. 1997), whereas the oldest historic lavas are from the eighteenth century CE (Viccaro and Cristofolini 2008). Nevertheless, some basal tholeiites (here termed "ancient Etna") and prehistoric (i.e., < ~ 250 ka) alkaline lavas from the eastern flank (Carter and Civetta 1977; Marty et al. 1994; D'Orazio et al. 1997; Tanguy et al. 1997; Tonarini et al. 2001; Corsaro et al. 2002) have been previously analysed, as have some of the older Plio-Pleistocene-age Iblean Plateau lavas (Fig. 1; Carter and Civetta 1977; Tonarini et al. 1996; Trua et al. 1998; Miller et al. 2017).

Several authors have discussed the isotopic evolution of the magma sources beneath Sicily and Mt. Etna (Marty et al. 1994; Tonarini et al. 2001; Corsaro and Pompilio 2004; Branca et al. 2008; Viccaro and Cristofolini 2008). Strontium, Nd, and Hf isotopic compositions of eruptive products from the Iblean Plateau and Mt. Etna show a broad temporal evolution from DMM-like (depleted MORB [mid-ocean-ridge basalt] mantle) for the Iblean Plateau toward BSE (bulk silicate Earth) for recent (< 130-year-old) eruptions. This has been interpreted by some authors as evidence for subduction of Ionian oceanic lithosphere beneath Mt. Etna and modification of the sub-Etna mantle by subduction-derived fluids (Gvirtzman and Nur 1999). Doglioni et al. (2001) and Gasperini et al. (2002) considered that differential slab rollback between the Sicilian and Ionian segments of the Apennines slab may have opened a slab window that has enabled upwelling and decompression partial melting of underlying asthenospheric mantle. Schiano et al. (2001) also suggested that subduction-derived fluids might be metasomatising the upwelling asthenospheric mantle beneath Mt. Etna. In contrast, Kamenetsky et al. (2007), Viccaro and Cristofolini (2008), Nicotra et al. (2013), Correale et al. (2014), Miller et al. (2017), and Viccaro and Zuccarello (2017) considered Etna's isotopic variation to be the result of melting of a heterogeneous mixture of mantle spinel lherzolites and pyroxenites.

In this paper we investigate prehistoric lavas from Mt. Etna that erupted during a poorly known period in the evolution of the volcano between ~ 85 and ~ 4 ka. The lavas are exposed in the southern wall of the Valle del Bove (latitude 15° 00′ 53″–15° 01′ 42″; longitude 37° 42′ 50″–37° 42′ 32″) and were collected in 1988 from four separate near-vertical sections (Fig. 1). They consist of several moderately evolved, geochemically distinct lava groups that correlate stratigraphically across the sections (Spence and Downes 2011). These lavas were previously considered to be products of a single eruptive centre referred to as "Vavalaci" (Lo Giudice 1970; McGuire 1982; Guest et al. 1984). They are now, however, reinterpreted as derived from several discrete volcanic centres dating from ~ 85 to ~ 4 ka (Calvari et al. 1994; De Beni et al. 2011; Branca et al. 2011a). Thus, they represent an ˜ 80 kyr time span between the older magmatism of Mt. Etna and

the present day, providing a link between the earlier eruptive phases and historic eruptions.

In this study, we provide new radiogenic isotope data (Sr, Nd, Pb, and Hf) for these prehistoric Valle del Bove units to investigate whether the broad trends in magma source evolution from ancient Etna eruptions to the modern day continued systematically throughout the ~ 80 kyr period that they cover. We also investigate whether variations in isotopic compositions are the result of melting of subducted Ionian oceanic lithosphere or rather a consequence of melting of ambient heterogeneous mantle.

Background and sampling

Mount Etna is located near the convergence of the African and Eurasian tectonic plates (Fig. 1a). North of Mt. Etna, the Quaternary Aeolian volcanic arc formed by northwards subduction of the Ionian oceanic plate. The Iblean Plateau, situated ~ 100 km south of Etna (Fig. 1a), represents the relatively undeformed foreland that was uplifted and underwent discontinuous intraplate volcanism during the Tertiary and Quaternary (Tonarini et al. 1996; Trua et al. 1998).

All samples for this study were collected from four stratigraphic sections in the southern wall of the Valle del Bove (Spence and Downes 2011). The sections from east to west are: Section A—Valle del Tripodo; Section D—west of Serra dell'Acqua; Section E—Serra Pirciata; and Section C—Serra Vavalaci (Fig. 1c). The stratigraphy, field relations, and petrography of the lavas can be inferred from the recent geological map of Etna by Branca et al. (2011b). In combination with the ^{40}Ar/^{39}Ar ages of De Beni et al. (2011) (Table 1), they comprise six discrete lithological units (Fig. 1d). From oldest to youngest, these are: (1) Salifizio-1; (2) Salifizio-2; (3) Cuvigghiuni; (4/5) the Valle del Tripodo member of the Piano Provenzana formation (Tripodo member) and Piano Provenzana; and (6) Mongibello. Note that we have tried to follow the terminology of Branca et al. (2011b), choosing terms from the geological map of Etna that was published after field sampling had been completed. However, we have inadvertently employed a mixture of terms relating to different volcanic centres (e.g., Cuvigghiuni, Mongibello) and lithostratigraphic units (e.g., Piano Provenzana, Tripodo). To improve clarity, Table 1 and the table legend at the bottom of Fig. 1 explain the equivalence between the terms used in this study and those of the geological map of Branca et al. (2011b).

The stratigraphically lowest lavas in sections A and D (Fig. 1c, d) are basaltic trachyandesites belonging to the Valle degli Zappini formation (Salifizio-1) and are therefore older than 85.6 ka. Basaltic trachyandesite lavas from the Serra del Salifizio formation (Salifizio-2), dated at 85.6 ± 6.8 ka, overlie this unit and are present in all

Table 1 Valle del Bove sections with associated lithostratigraphy and isotope age ranges

Recent (<130 yrs) & Historic (>130 yrs)

Synthemic units		Lithostratigraphic units		Volcanic Unit	Formation Name, Valle del Bove sections, this study			
					Section A	Section D	Section E	Section C
Stratovolcano Supersynthem	Il Piano Synthem	Torre del Filosofo f. Pietracannone f.	*Present*	**Mongibello** ▢			Pietracannone (lower member) (<15 ka)	Pietracannone (lower member) (<15 ka)
	Concazze Synthem	Portella Giumenta f. Monte Calvario f. Piano Provenzana f. Pizzi Deneri f. Serra della Concazze f.		Ellittico	**Tripodo member** (Piano Provenzana) (42-30 ka) ◆		**Piano Provenzana** (42-30 ka) ▲	
Valle del Bove Supersynthem	Zappini Synthem	Canalone della Montagnola f. Serra Cuvigghiuni f. Aqua della Rocca f. Serra del Salifizio f. Valle degli Zappini f. Serra Giannicola Grande f. Monte fior di Cosimo f. Monte Scorsone f.	*60 ka*	**Cuvigghiuni** ◇ **Salifizio-2** ● **Salifizio-1** ✕	Serra del Salifizio (85.6±6.8 ka) Valle degli Zappini (>85.6 ka)	Canalone della Montagnola (79-70 ka) Serra del Salifizio (85.6±6.8 ka) Valle degli Zappini (>85.6 ka)	Canalone della Montagnola (79-70 ka) Serra del Salifizio (85.6±6.8 ka)	Canalone della Montagnola (79-70 ka) Serra del Salifizio (85.6±6.8 ka)
	Croce Menza Synthem	Piano del Trifoglietto f. Rocche f. Contrada Passo Cannelli f.						
Timpe Supersynthem	S. Alfio Synthem	Valverde f. Moscarello f. Calanna f.	*110 ka*					
	Acireale Synthem	Timpa f. Timpa di Don Masi f.						
Basal Tholeiitic Supersynthem	Andrano Synthem	S. Maria di Licodia f.	*220 ka*					
	Aci Trezza Synthem	Aci Castello f.	*~500 ka*					

Prehistoric / Ancient

Formation designations, volcanic units, synthems, supersynthems and isotopic ages from Branca et al. (2011b) and adapted from DeBeni et al. (2011), Colour coding using above corresponds to that in subsequent figures

four sections (Table 1). Both formations are considered to belong to the Salifizio volcano (Branca et al. 2011b). The overlying trachybasalt and basaltic trachyandesite lavas in sections D, E, and C are from the Canalone della Montagnola formation, dated at 79–70 ka and defined by Branca et al. (2011b) as eruptions of the Cuvigghiuni volcano. The uppermost lavas in section A (Fig. 1c, d) are less evolved trachybasaltic lavas from the Tripodo member of the Piano Provenzana formation of the Ellittico volcano (Branca et al. 2011b), dated at 42–30 ka. In sections E and C, trachyandesitic lavas form the uppermost member of the Piano Provenzana formation, also dated at 42–30 ka. Precise age relationships between the Tripodo and upper Piano Provenzana members have not been determined (Branca et al. 2011b). We assume from field evidence (Spence and Downes 2011) that the upper member (Piano Provenzana) lavas are younger than those of Tripodo, but our conclusions are not affected by this assumption. The two units are mineralogically and texturally distinguishable and are also compositionally distinct. The basaltic trachyandesitic lavas at the top of sections E and C form the top of the southern wall of the Valle del Bove at the Schiena dell'Asino. These are products of the Mongibello

stratovolcano and are younger than 15 ka (Branca et al. 2011b; De Beni et al. 2011).

The sampled lavas are extremely fresh, and most are vesicular to highly vesicular (> 20%). They range from aphyric to strongly porphyritic (25–40% phenocrysts), with plagioclase as the most common phenocryst phase. Some of the larger plagioclase phenocrysts exhibit zoning and/or sieve textures. Clinopyroxene (augite) phenocrysts/megacrysts range up to 5 mm in size; they typically exhibit oscillatory zoning and ophitic textures, enclosing aligned plagioclase laths and FeTi oxides. Glomeroporphyritic aggregates of plagioclase, augite and Ti-magnetite are also common. Although its modal abundance is relatively low, olivine is present as phenocrysts and in the groundmass of all but the most evolved and aphyric lavas. Kaersutite occurs rarely as small, ragged and broken, partially reabsorbed crystals with reaction rims of titanomagnetite, indicating instability during low-pressure fractionation. Accessory apatite is also present as inclusions in augite and some plagioclase. Further details of sample petrography can be found in Spence and Downes (2011).

Sample preparation and methods

All the sampled Valle del Bove lavas were ground to a powder using a tungsten carbide mortar and analysed by X-Ray Fluorescence (XRF) at Royal Holloway University of London (Spence and Downes 2011). XRF data for ten of the samples were reported in Spence and Downes (2011), others are presented in Table 2. Strontium and Nd isotopic analyses were initially obtained on 11 samples at the University of London radiogenic isotope facility at Royal Holloway in the 1990s (data published in this study) but were unevenly distributed among the six lithostratigraphic units. Therefore, for the present study, 12 additional samples were analysed for Sr, Nd, Pb, and Hf isotopic ratios in other laboratories (see below for details).

Strontium and Nd isotopic ratios on the 11 samples analysed at Royal Holloway University of London (Table 3) were determined following the method described by Thirlwall (1991) and Thirlwall et al. (1997). Strontium and Nd isotopic compositions were determined multi-dynamically using a VG354 5-collector mass spectrometer, following conventional dissolution and chemical separation without prior sample leaching. Data were collected during several analytical sessions (methods in Thirlwall 1991), with reference materials reproducible to ± 0.000020 and ± 0.000008 (2SD) for $^{87}Sr/^{86}Sr$ and $^{143}Nd/^{144}Nd$, respectively. For a few samples, small machine bias-corrections were made based on the difference between the means of the measuring period for NIST SRM 987 and a Nd in-house standard. The machine bias corrections were never more than $+0.000009$ and -0.000006, respectively. The long-term laboratory averages for SRM 987 were $^{87}Sr/^{86}Sr = 0.710248$ and $^{143}Nd/^{144}Nd = 0.511420$ for the Nd house standard (equivalent to La Jolla of 0.511857; Thirlwall 1991). Measured Nd and Sr procedural blanks were not significant with respect to the sample concentrations.

The new Sr and Nd isotope analyses (Table 3) were carried out at the Department of Earth and Environmental Sciences, Ludwig-Maximilians-Universität of Munich, following the methods described in Hegner et al. (1995). No sample powder leaching was employed. Strontium and Nd isotopes were measured as metals on single W and double Re-filament configurations, respectively. Total procedural blanks of < 500 pg for Sr and < 100 pg for Nd are not significant for the processed amounts of Sr and Nd. Isotope analyses were performed on an upgraded MAT 261 multi-collector thermal ionisation mass spectrometer. Strontium isotope abundance ratios were measured with a dynamic double-collector routine, while Nd isotope compositions were measured using a dynamic triple-collector routine, with corrections made for interfering ^{87}Rb and

^{144}Sm. $^{87}Sr/^{86}Sr$ and $^{143}Nd/^{144}Nd$ ratios were normalised for instrumental mass bias relative to $^{86}Sr/^{88}Sr = 0.1194$ and $^{146}Nd/^{144}Nd = 0.7219$, using a Rayleigh fractionation law. During the period of this study the NIST SRM 987 Sr reference material yielded $^{87}Sr/^{86}Sr = 0.710234 \pm 0.000006$ (2SD of population, $n = 8$) and the La Jolla Nd reference material $^{143}Nd/^{144}Nd = 0.511847 \pm 0.000008$ (2SD of population, $n = 10$). The long-term external precision for $^{87}Sr/^{86}Sr$ and $^{143}Nd/^{144}Nd$ is estimated at ca. 1.1×10^{-5} (2SD).

The Pb and Hf isotope analyses (Table 3) were carried out at the Ecole Normale Supérieure in Lyon (ENSL) by solution chemistry (Hf only; Pb separated at University of New Hampshire; see below) and MC-ICP-MS (both Hf and Pb; Nu Plasma 500 HR) following the methods of Blichert-Toft et al. (1997) and Blichert-Toft and Albarède (2009). $^{176}Hf/^{177}Hf$ ratios were corrected for instrumental mass fractionation relative to $^{179}Hf/^{177}Hf = 0.7325$ using an exponential law. The JMC-475 Hf standard was run every two samples and averaged 0.282163 ± 0.000007 (2σ; $n = 14$) for $^{176}Hf/^{177}Hf$ during the single run session of this work. Since this is identical to the accepted value of 0.282163 ± 0.000009 (Blichert-Toft et al. 1997) for JMC-475, no corrections were applied to the data. ε_{Hf} values (Table 3) were calculated using $^{176}Hf/^{177}Hf = 0.282772$ (Blichert-Toft and Albarède 1997).

Samples were prepared for Pb isotope analyses at the University of New Hampshire (UNH) geochemical laboratories. Samples were first leached in hot 6 M HCl to remove surficial contaminants. Lead was then isolated from the sample following procedures adapted from Bryce and DePaolo (2004). The Pb isotope data obtained by MC-ICP-MS at the Ecole Normale Supérieure in Lyon were corrected for instrumental mass fractionation by thallium normalization and adjusted for machine drift by sample-standard bracketing (White et al. 2000; Albarède et al. 2004) using the values of Eisele et al. (2003) for NIST SRM 981. Three NIST SRM 981 standard analyses run within the bracketed sample suite yielded results (with external reproducibility) of $^{208}Pb/^{204}Pb = 36.726(4)$ $^{207}Pb/^{204}Pb = 15.498(3)$, and $^{206}Pb/^{204}Pb = 16.941(3)$. Total procedural Hf and Pb blanks were < 20 pg and < 100 pg, respectively, negligible relative to the abundances of these elements processed for study.

Results

Valle del Bove lavas are moderately evolved (50–62 wt% SiO_2, Fig. 2a) and, based on the ratio of Na_2O to K_2O (1.9–2.8), the rocks are mildly sodic basaltic trachy-andesites and trachyandesites, including one trachyte sample. Figure 2a also shows fields that encompass the range of compositions for recent (i.e., < 130-years old) and historic

Table 2 Major and trace element concentrations of the Valle del Bove samples

	Section A: Valle del Tripodo				Section D: West of Serra dell' Acqua						Section E:	
	A1[a]	A14[d]	A15[d]	A18b[d]	D5[a]	D8[a]	D10[a]	D12[a]	D13[a]	D21[c]	E2[b]	E7[c]
SiO_2	57.57	50.37	50.55	51.14	53.89	53.30	53.79	56.22	52.59	54.51	53.78	51.22
TiO_2	0.87	1.49	1.50	1.35	1.08	1.10	1.20	0.98	1.20	0.93	1.05	1.27
Al_2O_3	19.36	17.41	17.61	20.33	18.14	18.00	18.48	18.46	18.55	18.52	18.29	19.13
Fe_2O_3	5.85	9.23	9.26	7.96	7.78	7.95	7.69	7.09	8.29	7.46	8.06	8.87
MnO	0.12	0.17	0.17	0.17	0.15	0.14	0.14	0.15	0.15	0.16	0.16	0.16
MgO	1.95	4.76	4.86	2.84	4.06	4.42	3.44	2.86	4.03	2.82	3.45	3.72
CaO	5.84	8.17	8.10	8.69	7.93	8.29	7.56	6.44	8.50	6.66	7.27	8.08
Na_2O	5.59	4.96	4.72	4.83	4.72	4.53	4.83	5.21	4.60	5.37	5.10	4.57
K_2O	2.58	2.17	2.18	1.70	1.97	1.85	1.96	2.40	1.77	2.49	2.19	1.96
P_2O_5	0.40	0.77	0.77	0.68	0.45	0.45	0.46	0.45	0.44	0.56	0.51	0.57
LOI	0.07	−0.20	−0.07	−0.09	0.07	−0.20	−0.11	−0.18	−0.40	0.17	−0.20	0.18
Total	100.21	99.29	99.64	99.59	100.24	99.83	99.44	100.08	99.71	99.66	99.67	99.74
Mg #	43	54	54	45	54	56	42	48	52	46	49	49
Rb	66	52	53	29	46	42	46	65	42	69	60	47
Sr	976	1143	1156	1662	1030	1042	1034	1019	1164	1192	1159	1403
Ba	953	877	881	943	746	723	750	919	768	1030	898	843
La	90	96	96	80	70	73	72	84	67	98	86	79
Ce	152	179	179	152	124	128	125	147	122	170	152	149
Nd	50	67	67	63	47	48	47	51	48	57	52	57
Zr	324	296	299	223	224	213	236	295	206	345	311	272
Nb	82	100	102	63	56	54	60	74	51	98	81	80
Y	26	30	29	29	23	24	26	25	25	27	25	26
Th	21	19	19	12	15	14	15	21	12	22	19	13

	Serra Pirciata			Section C: Serra Vavalaci							
	E8[c]	E11[e]	E13[f]	C7[c]	C19[e]	C21[e]	C22[e]	C24[f]	C25[f]	C26[f]	C27[f]
SiO_2	51.93	59.98	54.74	51.72	58.50	59.24	62.47	54.57	55.64	55.61	55.87
TiO_2	1.19	1.39	1.62	1.22	1.44	1.35	1.12	1.61	1.55	1.55	1.40
Al_2O_3	19.75	16.93	17.24	18.28	17.44	17.12	16.78	17.28	17.52	17.50	18.03
Fe_2O_3	8.14	6.02	8.36	8.61	6.64	6.59	5.10	8.40	7.48	7.52	6.84
MnO	0.16	0.17	0.20	0.17	0.17	0.17	0.16	0.20	0.21	0.21	0.21
MgO	3.04	1.76	2.61	4.33	2.12	2.01	1.44	2.62	2.27	2.31	2.29
CaO	7.63	3.74	5.70	8.06	4.78	4.49	3.01	5.70	4.80	4.83	4.94
Na_2O	5.30	5.94	5.66	4.77	5.75	5.86	6.27	5.56	6.63	6.54	6.51
K_2O	2.04	3.20	2.69	1.99	2.77	2.70	3.27	2.67	2.82	2.83	2.99
P_2O_5	0.64	0.46	0.79	0.53	0.62	0.60	0.35	0.79	0.63	0.62	0.60
LOI	−0.06	−0.04	−0.33	−0.08	0.00	−0.17	−0.01	−0.33	−0.06	−0.01	0.03
Total	99.75	99.55	99.28	99.59	100.23	99.96	99.96	99.07	99.48	99.52	99.71
Mg #	46	40	41	53	42	41	39	41	41	41	43
Rb	53	70	47	50	56	63	71	48	57	58	68
Sr	1460	787	1092	1211	995	995	726	1091	1029	1033	1016
Ba	909	1366	1291	817	1249	1242	1425	1277	1335	1342	1387
La	81	131	124	73	120	111	136	118	117	117	133
Ce	151	243	227	135	222	208	245	226	220	221	244
Nd	56	93	89	51	86	80	92	89	87	86	88
Zr	283	439	378	276	414	413	508	378	389	391	430
Nb	83	121	105	72	104	102	121	105	109	110	131
Y	26	46	42	24	42	38	49	39	43	43	42

Table 2 (continued)

	Serra Pirciata			Section C: Serra Vavalaci							
	E8[c]	E11[e]	E13[f]	C7[c]	C19[e]	C21[e]	C22[e]	C24[f]	C25[f]	C26[f]	C27[f]
Th	15	24	21	14	21	20	26	21	21	21	28

Major-element concentrations in wt%; trace elements in μg/g. Mg # calculated as $[Mg/(Mg + 0.9Fe)] \times 100$

[a] Salifizio-1

[b] Salifizio-2

[c] Cuvigghiuni

[d] Tripodo Member

[e] Piano Provenzana

[f] Mongibello

(i.e., > 130-years old) Etna lavas, along with the field for prehistoric and ancient Etna magmatic products. The Valle del Bove lavas overlap the field for previously analysed prehistoric and ancient Etna lavas, but most of these rocks, including Valle del Bove, have higher concentrations of SiO_2 and total alkalis than recent and historic Etna lavas. In a K_2O versus SiO_2 discrimination diagram (Fig. 2b) (Peccerillo and Taylor 1976) most Etna rock samples, including Valle del Bove, fall within the high-K field. Recent Etna samples, however, are distinct, being more enriched in K_2O for a given SiO_2 concentration than all other Etna lavas, as shown previously by Clocchiatti et al. (1988). Within the Valle del Bove suite, samples from Salifizio-1 and Piano Provenzana have consistently lower concentrations of K_2O and total alkalis for a given SiO_2 concentration than those of Salifizio-2, Cuvigghiuni, the Tripodo member, or Mongibello.

Although the higher SiO_2 concentrations for prehistoric and ancient Etna samples suggest that these rocks are all more evolved than recent and historic Etna samples, plots of major element oxides versus MgO (Fig. 3) show that the least evolved lavas from Valle del Bove, particularly those from Salifizio-1, have similar MgO concentrations (and Mg numbers; see Online Resource 1, Fig. S1) to recent and historic Etna, suggesting similar degrees of magmatic evolution. Valle del Bove lavas are distinct in having higher SiO_2 for a given MgO concentration (Fig. 3a). They also have lower CaO, Al_2O_3, TiO_2, and $FeO_{total.}$ concentrations and CaO/Al_2O_3 ratios. Recent Etna lavas have significantly higher K_2O for a given MgO concentration (see Online Resource 1, Fig. S1) than either historic or ancient/prehistoric Etna, including the Valle del Bove lavas, consistent with their higher K_2O shown in Fig. 2b. Only two samples from the Tripodo member, A14 and A15 (Table 2), are as enriched in K_2O at similar MgO concentration as recent Etna lavas. Other samples from the Tripodo member are more evolved (MgO < 3.3 wt%), yet they have lower K_2O concentrations, i.e., opposite of what would be expected from fractional crystallisation of the observed phenocryst phases. Samples A14 and A15 occur stratigraphically below

the more evolved Tripodo member samples and below a 20 m interval with lack of exposure (Spence and Downes 2011); hence, the relationship between these two groups of Tripodo samples is unclear, but they may not be petrogenetically related.

The Valle del Bove lavas overlap the compositional fields for ancient and prehistoric Etna in Fig. 3, with a few notable exceptions. Salifizio-1 lavas, the oldest rocks in the suite, have SiO_2 concentrations higher than those of recent and historic Etna, but also higher than most other ancient and prehistoric Etna rocks (Fig. 3a). They also have lower Al_2O_3 and TiO_2 (Fig. 3c, e). Ancient and prehistoric Etna samples, including those from Valle del Bove, extend to more evolved compositions (i.e., lower MgO and higher SiO_2) than recent or historic Etna lavas.

Figure 4a shows the primitive-mantle-normalised incompatible element patterns for the Valle del Bove samples compared with those of ocean island basalts (OIB) representative of EM (enriched mantle) and HIMU (mantle with high time-integrated U/Pb) sources, as well as average global subducted sediments (GLOSS) and bulk continental crust. Figure 4b shows the data normalised to the composition of average recent Etna lavas. All Valle del Bove samples are enriched in most of the incompatible trace elements relative to recent and historic Etna basalts (Fig. 4b). Two units (Mongibello and Piano Provenzana) exhibit particular enrichment in nearly all incompatible trace elements except Sr and Ti, consistent with their evolved compositions (MgO concentrations < 2.6 wt%, Table 2; see also Figs. 2 and 3). In contrast, the least evolved samples (e.g., from Salifizio-1 and the Tripodo member) have compositions typical of intraplate alkaline magmas, e.g., OIB-like, although with relative enrichments in Ba, Th, and Pb and depletions in Ti and K (Fig. 4a). Of note in this context are the high La/Nb ratios relative to average OIB compositions. The Tripodo member has a trace element pattern that is distinct from most other Valle del Bove units. It is more akin to historic Etna, particularly in terms of its low Th/Nb and Th/Ba ratios (Fig. 4b). However, the least-evolved Tripodo samples, A14 and A15,
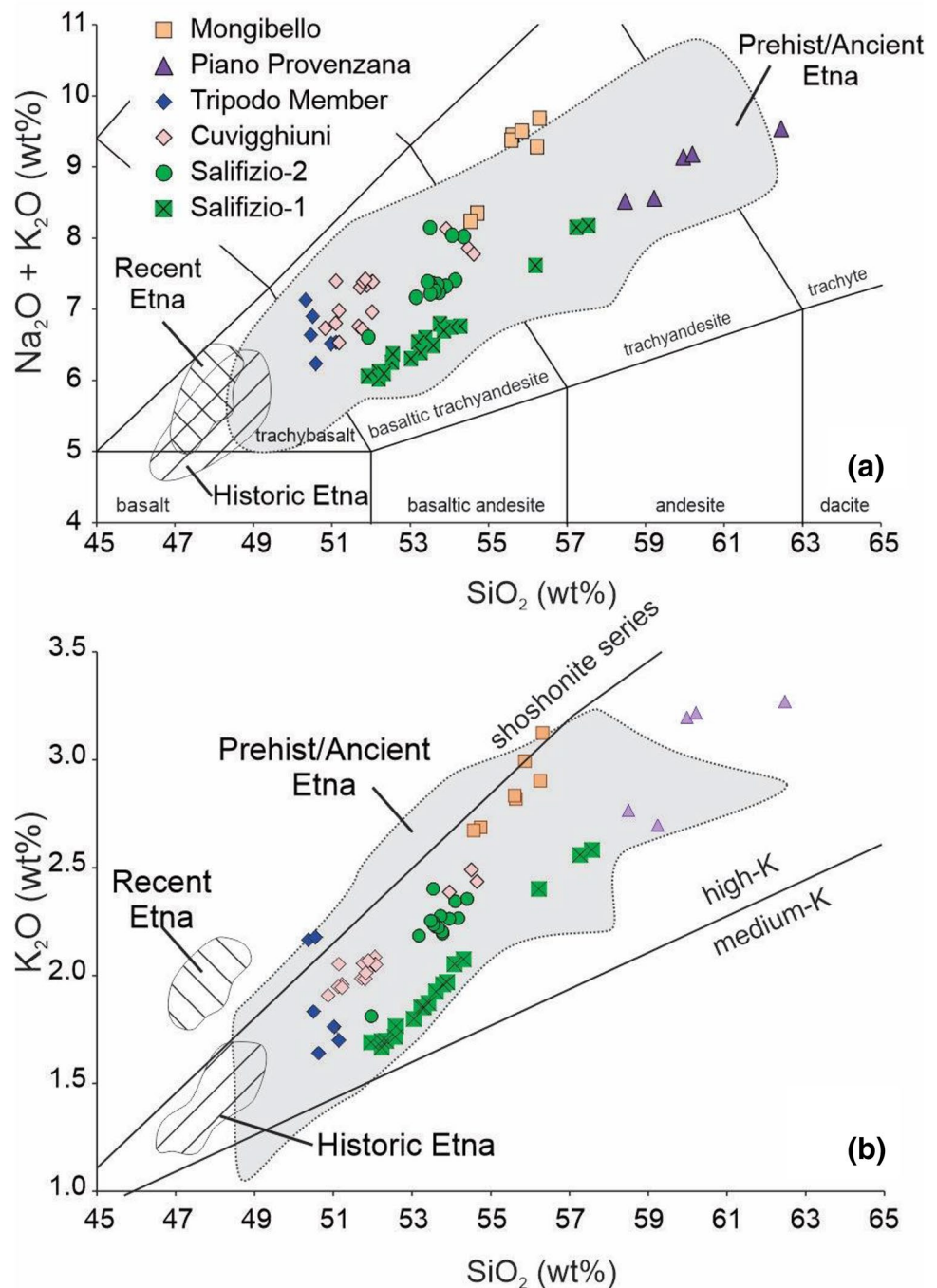
Table 3 Isotopic compositions of the Valle del Bove samples

	Section A: Valle del Tripodo				Section D: West of Serra dell' Acqua						Section E	
	A1[a,1,2]	A14[d,3]	A15[d,1,2]	A18b[d,3]	D5[a,1,2]	D8[a,3]	D10[a,3]	D12[a,1,2]	D13[a,3]	D21[c,1,2]	E2[b,3]	E7[c,1,2]
$^{87}Sr/^{86}Sr$	0.703640±07	0.703336±11	0.703335±09	0.703414±07	0.703556±06	0.703546±10	0.703597±08	0.703544±08	0.703534±08	0.703396±08	0.703393±13	0.703421±08
ε Sr	−12.2	−16.5	−16.5	−15.4	−13.4	−13.5	−12.8	−13.6	−13.7	−15.7	−15.7	−15.3
$^{143}Nd/^{144}Nd$	0.512837±09	0.512902±04	0.512906±11	0.512893±06	0.512868±10	0.512872±06	0.512864±06	0.512876±08	0.512871±04	0.512908±09	0.512900±05	0.512907±11
ε Nd	4.0	5.3	5.4	5.1	4.6	4.7	4.6	4.8	4.7	5.4	5.3	5.4
$^{176}Hf/^{177}Hf$	0.282931±04		0.282954±04		0.282956±03			0.282949±03		0.282978±04		0.282972±04
ε Hf	5.6		6.4		6.5			6.3		7.3		7.1
$^{206}Pb/^{204}Pb$	19.827		20.027		19.941			20.002		19.859		19.973
$^{207}Pb/^{204}Pb$	15.681		15.682		15.680			15.677		15.673		15.677
$^{208}Pb/^{204}Pb$	39.575		39.681		39.632			39.660		39.633		39.635

	Section E; Serra Pirciata (cont)			Section C: Serra Vavalaci							
	E8[c,3]	E11[e,1,2]	E13[f,3]	C7[c,3]	C19[e,1,2]	C21[e,3]	C22[e,1,2]	C24[f,1,2]	C25[f,1,2]	C26[f,1,2]	C27[f,3]
$^{87}Sr/^{86}Sr$	0.703390±09	0.703470±08	0.703410±11	0.703372±17	0.703467±08	0.703480±10	0.703482±07	0.703421±08	0.703404±07	0.703391±09	0.703348±07
ε Sr	−15.8	−14.6	−15.5	−16.0	−14.7	−14.5	−14.5	−15.3	−15.6	−15.7	−16.4
$^{143}Nd/^{144}Nd$	0.512908±06	0.512865±11	0.512886±06	0.512903±07	0.512846±11	0.512848±05	0.512847±09	0.512896±11	0.512904±10	0.512905±09	0.512897±07
ε Nd	5.4	4.6	5.0	5.3	4.2	4.3	4.2	5.2	5.3	5.4	5.2
$^{176}Hf/^{177}Hf$		0.282883±03			0.282886±05		0.282877±04	0.282940±03	0.282974±04	0.282970±04	
ε Hf		3.9			4.0		3.7	5.9	7.2	7.0	
$^{206}Pb/^{204}Pb$		19.803			19.795		19.764	19.946	20.021	20.023	
$^{207}Pb/^{204}Pb$		15.680			15.681		15.674	15.677	15.674	15.676	
$^{208}Pb/^{204}Pb$		39.548			39.551		39.521	39.629	39.667	39.672	

[a]Salifizio–1; [b]Salifizio–2; [c]Cuvigghiuni; [d]Tripodo Member; [e]Piano Provenzana; [f]Mongibello

[1]Sr and Nd isotopic analyses by E. Hegner, analyzed at LMU; [2] Hf and Pb isotopic analyses by J. Blichert-Toft and J. Bryce, analyzed at ENSL and UNH; [3]Sr and Nd isotopic analyses by P.Z. Vroon, analyzed at RHUL. Errors of isotopic ratios are 2σ mean and refer to the last digits of the ratios. ε Nd and ε Hf calculated using the parameters of Bouvier et al. (2008) and Blichert-Toft and Albarède (1997), respectively

have higher concentrations of nearly all incompatible trace elements (Table 2) than the most-evolved samples, further supporting the idea that these two groups of samples are not related by fractional crystallisation.

The Valle del Bove lavas show significant variations in $^{87}Sr/^{86}Sr$ (0.70334–0.70364), $^{143}Nd/^{144}Nd$ (0.51284–0.51290), $^{176}Hf/^{177}Hf$ (0.28288–0.28298), and $^{206}Pb/^{204}Pb$ (19.76–20.03) ratios with clear differences between the six units (Fig. 5). Samples from the oldest unit (Salifizio-1) have the highest $^{87}Sr/^{86}Sr$ ratios of all the Valle del Bove units (> 0.7035). These rocks contrast with those of similar age from the northern wall of the Valle del Bove, i.e., the Rocca Capra (ca. 81–78 ka) (D'Orazio et al. 1997) and the prehistoric/ancient Etna rocks reported by Marty et al. (1994), all of which have $^{87}Sr/^{86}Sr$ ratios < 0.70325 and $^{143}Nd/^{144}Nd$ > 0.51291. Instead, Salifizio-1 samples overlap the field of recent high-$^{87}Sr/^{86}Sr$ Etna lavas (Fig. 5a, b) in a Sr–Nd isotope diagram. They also have overlapping to lower $^{176}Hf/^{177}Hf$ and $^{143}Nd/^{144}Nd$ ratios relative to recent Etna lavas (Fig. 5c, e). Their Hf isotopic compositions overlap
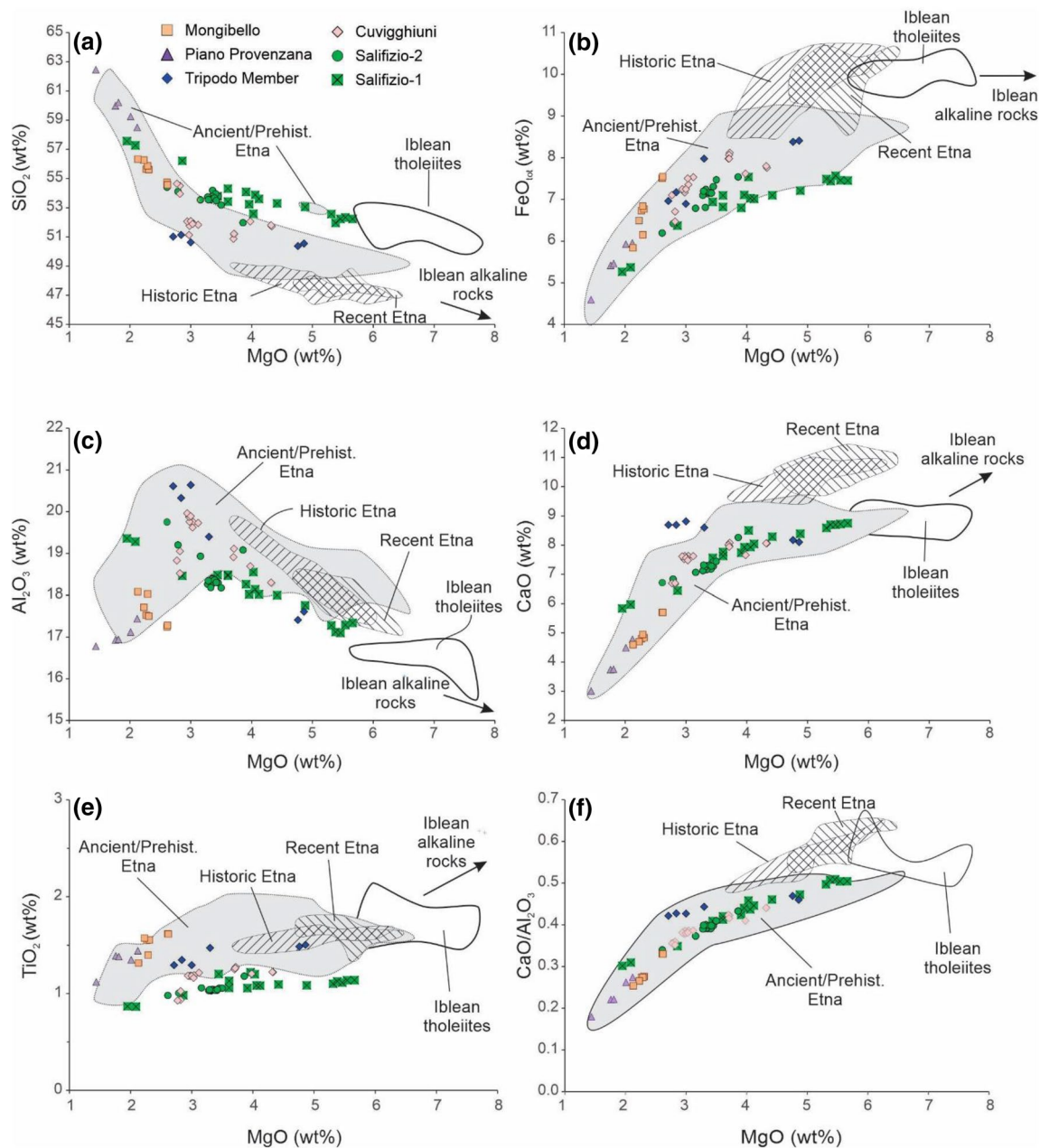
Fig. 3 Major element variation diagrams for **a** SiO$_2$, **b** FeO$_{total}$, **c** Al$_2$O$_3$, **d** CaO, **e** TiO$_2$, and **f** CaO/Al$_2$O$_3$ versus MgO wt%. Data sources for ancient to recent Etna magmatism as in Fig. 2. Data for Iblean Plateau tholeiites from Tonarini et al. (1996) and Trua et al. (1998)

those of most younger Valle del Bove units (except Piano Provenzana), but their ^{143}Nd/^{144}Nd ratios are lower. Thus, the isotopic data suggest that Salifizio-1 magmas were derived from a source isotopically similar to that of recent Etna magmas and distinct from that of other ancient and prehistoric Etna rocks. In contrast, the slightly younger (~85–70 ka) Salifizio-2 and Cuvigghiuni lavas have lower ^{87}Sr/^{86}Sr and higher ^{176}Hf/^{177}Hf ratios and plot within or near the field of historic Etna lavas (Fig. 5a, c, e), as do lavas from the Tripodo member. However, even these samples have higher

^{87}Sr/^{86}Sr ratios than most samples of ancient and prehistoric Etna (Marty et al. 1994; D'Orazio et al. 1997). All VdB units, however, have lower ^{87}Sr/^{86}Sr ratios than the unusual prehistoric picrite, FS (pyroclastic fall deposit), analysed by Correale et al. (2014). The higher Sr isotopic ratio for this sample (0.70391) was attributed to crustal contamination, although the authors did not distinguish between contamination occurring in a shallow crustal magma chamber or via subduction modification of the mantle source.
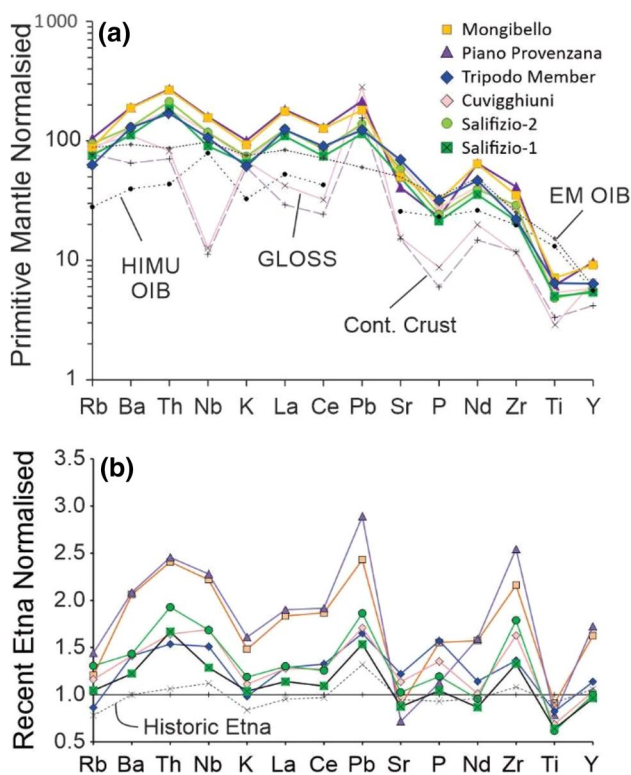
Fig. 4 Primitive-mantle-normalised incompatible element diagram (normalising values from Sun and McDonough 1989) for the six Valle del Bove units and historic and recent Etna. GLOSS (= global subducted sediment) average from Plank and Langmuir (1998); bulk continental crust average from Rudnick and Gao (2003). Representative EM OIB and HIMU OIB based on average compositions of St. Helena and Tristan da Cunha from Willbold and Stracke (2006). **b** Recent-Etna-normalised incompatible element diagram for the six Valle del Bove units. The Mongibello and Piano Provenzana lavas are the most highly enriched in LILE and HFSE (high field-strength elements) compared to average recent eruptions. Data sources as in Fig. 2

The Piano Provenzana lavas have the lowest ^{176}Hf/^{177}Hf ratios of all the analysed prehistoric lavas and almost lowest ^{143}Nd/^{144}Nd (the Nd isotope values overlap those of Salifizio-1). The youngest Mongibello lavas return to isotopic ratios that are more typical of historic Etna, with higher ^{143}Nd/^{144}Nd (Fig. 5b, d, f). The Hf and Sr isotopic compositions thus indicate the existence of at least three different components, two of which are predominant, i.e., the isotopically distinct sources of recent Etna lavas and historic/prehistoric Etna lavas, with five of the six Valle del Bove units overlapping these two fields. The third component, with an unusually low Hf isotopic composition for a given Sr or Nd isotopic composition, is seen only in the Piano Provenzana unit (Fig. 5c, e). This component has not previously been observed in samples from Mt. Etna, regardless of eruption age or major element composition.

Strontium, Nd, and Hf isotopic ratios (Fig. 5) show a change over time from more depleted DMM-like compositions (e.g., ε$_{Nd}$ of ~ +10) for ancient Iblean tholeiites to less depleted isotopic compositions for recent Etna eruptions. However, this simple trend breaks down during the ~ 80 kyr time span of the Valle del Bove eruptions (Fig. 5). Instead, a wider range of compositions appears to have been available for prehistoric Etna than exists today, in particular with addition of the new data of this study for Salifizio-1 and Piano Provenzana.

Lead isotope data for lavas from the Iblean Plateau and Mt. Etna (Fig. 6) also show a trend from depleted towards more enriched source compositions over time. However, some of the variation in the literature data, particularly in ^{207}Pb/^{204}Pb, may result, in part, from the greater analytical uncertainty of the older data collected using thermal ionisation mass spectrometry as compared with modern MC-ICP-MS data, which better control instrumental mass discrimination. There may also be some differences in sample preparation, particularly with regards to whether pre-dissolution leaching was applied. Lead isotope compositions of the Valle del Bove samples analysed using MC-ICP-MS with Tl-normalisation and sample-standard bracketing show tight linearity in Pb isotope space over the ~ 80 kyr time span considered (Fig. 6). The Valle del Bove units have relatively radiogenic Pb isotope compositions, overlapping the fields for recent, historic, and prehistoric/ancient Etna, and extending to higher ^{206}Pb/^{204}Pb and ^{208}Pb/^{204}Pb ratios than those from the Iblean Plateau. Among the Valle del Bove units, the Piano Provenzana lavas have the lowest ^{206}Pb/^{204}Pb (19.76–19.80), whereas the Tripodo member is the most radiogenic (i.e., its source shows the highest time-integrated U/Pb of all samples). The radiogenic Pb isotope composition of the Tripodo member contrasts with its lower ^{87}Sr/^{86}Sr than in the other samples (Fig. 5a), which suggests a source that is more incompatible element depleted (i.e., time-integrated depletion in Rb relative to Sr) than that of most other Valle del Bove lavas.

Discussion

Fractionation of Valle del Bove prehistoric magmas

The data points in the TAS diagram (Fig. 2a) suggest that most of the prehistoric Valle del Bove lavas are more evolved than recent and historic Etna eruptions (Tanguy et al. 1997), with the Mongibello and Piano Provenzana lavas amongst the most evolved. Salifizio-1 and Piano Provenzana lavas exhibit lower concentrations of total alkalis for a given SiO$_2$ concentration and are transitional to silica oversaturated in composition (i.e., up to 4.3 wt% normative quartz), whereas the Mongibello lavas are all silica undersaturated, with up
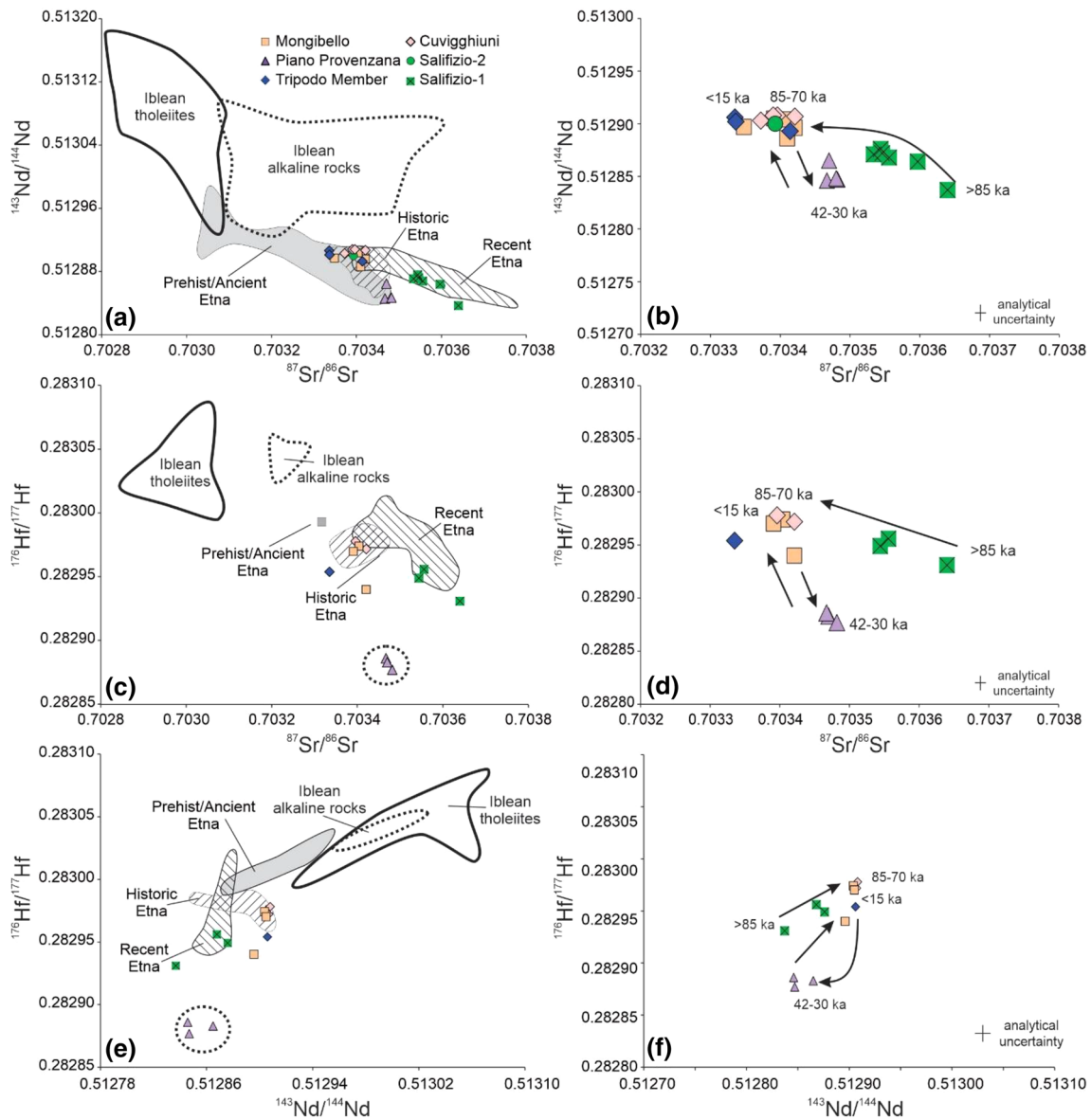
Fig. 5 **a** $^{143}Nd/^{144}Nd$ versus $^{87}Sr/^{86}Sr$, **c** $^{176}Hf/^{177}Hf$ versus $^{87}Sr/^{86}Sr$, and **e** $^{176}Hf/^{177}Hf$ versus $^{143}Nd/^{144}Nd$ ratios for the six Valle del Bove units, compared with data from the literature for prehistoric/ancient, historic, and recent lavas from Etna and tholeiitic and alkali lavas from the Iblean Plateau. Five of the 6 units fall within the fields for recent and historic Etna lavas, whereas the Piano Provenzana unit (encircled) lies outside of these fields. Data sources for Nd and Sr isotopic compositions of recent Etna samples from Armienti et al. (1989), Marty et al. (1994), Tonarini et al. (1995, 2001), and Viccaro and Cristofolini (2008). Historic Etna data from Marty et al. (1994), Tonarini et al. (2001), and Viccaro and Cristofolini (2008). Ancient/prehistoric Etna data from D'Orazio et al. (1997) and Marty et al. (1994). Iblean Plateau data from Tonarini et al. (1996) and Trua et al.

(1998). Hafnium isotopic ratios for historic and recent Etna from Viccaro et al. (2011), and for prehistoric Etna and Iblean Plateau from Gasperini et al. (2002), Miller et al. (2017), and Kempton (unpublished). The unusual prehistoric (3930 ± 60 years BP; Coltelli et al. 2005) picrite sample, FS, plots outside the range of Sr isotope values shown in **a**, with an $^{87}Sr/^{86}Sr$ ratio of 0.70391 (Correale et al. 2014); its $^{143}Nd/^{144}Nd$ ratio, however, overlaps the field for prehistoric/ancient Etna as shown. **b**, **d**, and **f** show isotopic compositions for the six Valle del Bove units from this study. Arrows and dates indicate temporal trends in Nd and Sr isotopic ratios for the six units over their ~ 80 kyr eruption period. Analytical uncertainties (2SD) for Valle del Bove data in **a**, **c**, and **e** are within the size of the symbols; analytical uncertainties (2SD) in **b**, **d**, and **f** are as shown by the error bars

to 6 wt% normative nepheline (see Online Resource 1, Fig. S2a). The lavas from Mongibello and Piano Provenzana are clearly the most evolved of the Valle del Bove samples, with Differentiation Indices (DI = normative q + or + ab + ne + lc)

of 63–77 (Fig. S2a), but they lie along two different differentiation trends (Fig. S2b). Samples from the Tripodo member, Cuvigghiuni, Salifizio-2, and Mongibello become more silica undersaturated as they become more evolved, whereas,
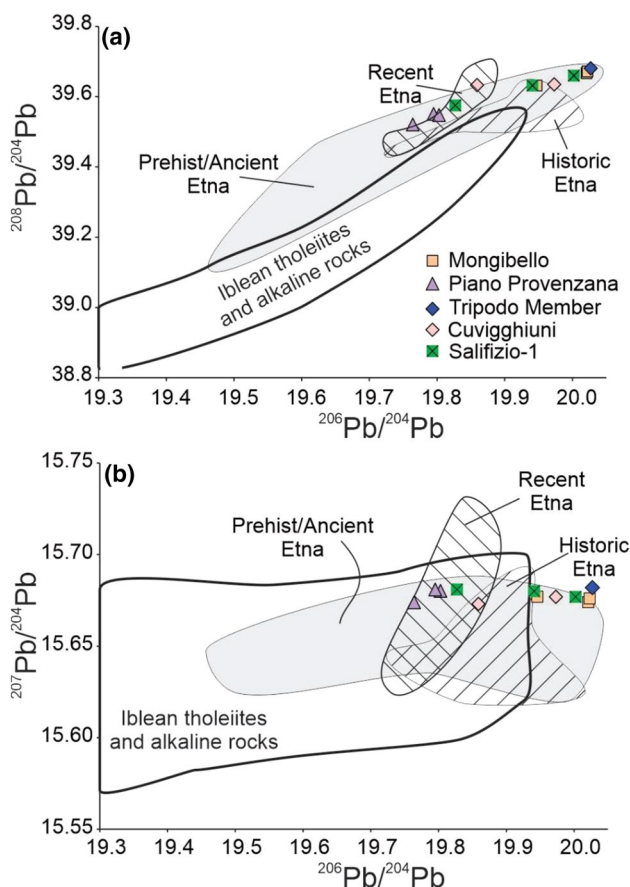
Fig. 6 a $^{208}Pb/^{204}Pb$ versus $^{206}Pb/^{204}Pb$ and **b** $^{207}Pb/^{204}Pb$ versus $^{206}Pb/^{204}Pb$ ratios for the six Valle del Bove units; prehistoric/ancient, historic, and recent Etna lavas; and tholeiitic and alkali lavas from the Iblean Plateau. Data for historic and recent Etna lavas from Carter and Civetta (1977) and Viccaro and Cristofolini (2008). Prehistoric/ancient Etna data from Carter and Civetta (1977) and Miller et al. (2017). Data for Iblean tholeiitic and alkali lavas from Carter and Civetta (1977), Tonarini et al. (1996), and Trua et al. (1998). Analytical uncertainties (2SD) for Valle del Bove data are within the size of the symbols

those from Salifizio-1 and Piano Provenzana become more silica saturated as differentiation increases.

To better understand the effects of fractional crystallisation on the Valle del Bove lavas, we have modelled isobaric fractionation using alphaMELTS 1.9 (Ghiorso and Sack 1995; Asimow and Ghiorso 1998; Smith and Asimow 2005). The results are shown in diagrams of MgO versus major element oxides SiO_2, Al_2O_3, CaO, FeO_{total}, as well as $Na_2O + K_2O$ versus SiO_2 (Fig. 7); details of the calculations are provided in Online Resource 2. Given the observation that the Valle del Bove suite includes at least two distinct differentiation trends, two different parental compositions have been assumed, one to represent the trend of increasing silica saturation (i.e., Salifizio-1 sample A5; Spence and Downes 2011) and the other to represent the trend of

increasing silica undersaturation with increased differentiation (i.e., Tripodo member sample A15; Table 2). Figure 7 shows that, for both starting compositions, fractional crystallisation at low pressure (i.e., 1 kb or ~ 3 km) fails to reproduce the data, in particular the observed increase in Al_2O_3 and decreasing FeO_{total} with decreasing MgO concentration. It also fails to reproduce the distribution of data on the TAS diagram (Fig. 7i, j), with low-pressure fractionation resulting in excessive enrichment in total alkalis. For these low-pressure calculations, we assumed 'dry' conditions (H_2O of 0.01 wt%), because of the low loss on ignition of the studied samples (Table 2). However, even if we assume higher water concentrations (e.g., 2 wt%), the model curves at low pressure (not shown) do not reproduce the data, in particular for Al_2O_3, FeO_{total}, and total alkalis.

In contrast, at moderate pressure (3.5 to 4 kb or ~ 10–12 km) and H_2O concentrations in the melt of ~ 3–4 wt%, the model curves reproduce the shape of the observed data distributions well. The difference in the residual melt pathways for low vs. moderate pressure is due to the expansion of the olivine stability field as pressure increases. At low pressures, plagioclase is the liquidus phase, followed by olivine and clinopyroxene in fairly rapid succession (see Online Resources 2 for details). The early stabilisation of plagioclase leads to a rapid depletion in Al_2O_3 as fractionation proceeds. At higher pressures, the olivine stability field expands, and the crystallisation sequence is typically spinel followed by olivine, followed closely by clinopyroxene, with plagioclase appearing much later. Under these conditions, Al_2O_3 increases until plagioclase starts to fractionate.

None of the models accurately reproduce the high Al_2O_3 concentrations of some samples from Cuvigghiuni and the Tripodo member (Fig. 7c, d). The MELTS models also fail to reproduce the variations in TiO_2 versus MgO (not shown). These discrepancies may, in part, be a function of uncertainties in the thermodynamic data used in the MELTS calculations and are associated with an over-stabilisation of spinel, a recognised problem of the MELTS software (Ghiorso et al. 2002). This leads to depletion in Al_2O_3, FeO, and TiO_2 in the calculated melts in excess of that in the actual rocks. Nonetheless, some of the Valle del Bove samples are plagioclase-rich, in particular the Tripodo lavas (Spence and Downes 2011). Hence, some of the observed compositional variation, particularly the enrichment in Al_2O_3, may be due to plagioclase accumulation at low pressures prior to eruption.

In summary, modelling with alphaMELTS 1.9 indicates that fractionation of the Valle del Bove lavas occurred in a magma chamber at moderate depths of ~ 10–12 km, which is consistent with interpretations based on geophysical data for the depth of present-day magma storage (Paonita et al. 2012; Mollo et al. 2015; Miller et al. 2017; Cannata et al. 2018). For the Valle del Bove lavas, fractionation is dominated by olivine and clinopyroxene. This contrasts with models for

Fig. 7 Major element variation diagrams for **a** SiO₂, **b** FeO_total, **c** Al₂O₃, **d** CaO, **e** K₂O, and **f** TiO₂ versus MgO wt% showing fractional crystallisation pathways calculated using alphaMELTS 1.9. Details of calculations in Online Resources 2. **a**, **c**, **e**, **g**, and **i** assume a starting composition of Salifizio-1 lava A5. **b**, **d**, **f**, **h**, and **j** assume Tripodo member A15 as the starting composition. Three model scenarios are presented for both starting compositions: (1) 1 kb, QFM, 'dry'; (2) 3.5 kb, QFM, 4 wt% H₂O; (3) 4 kb, NNO, 3 wt% H₂O. Data sources for recent, historic, and ancient Etna as in Fig. 3
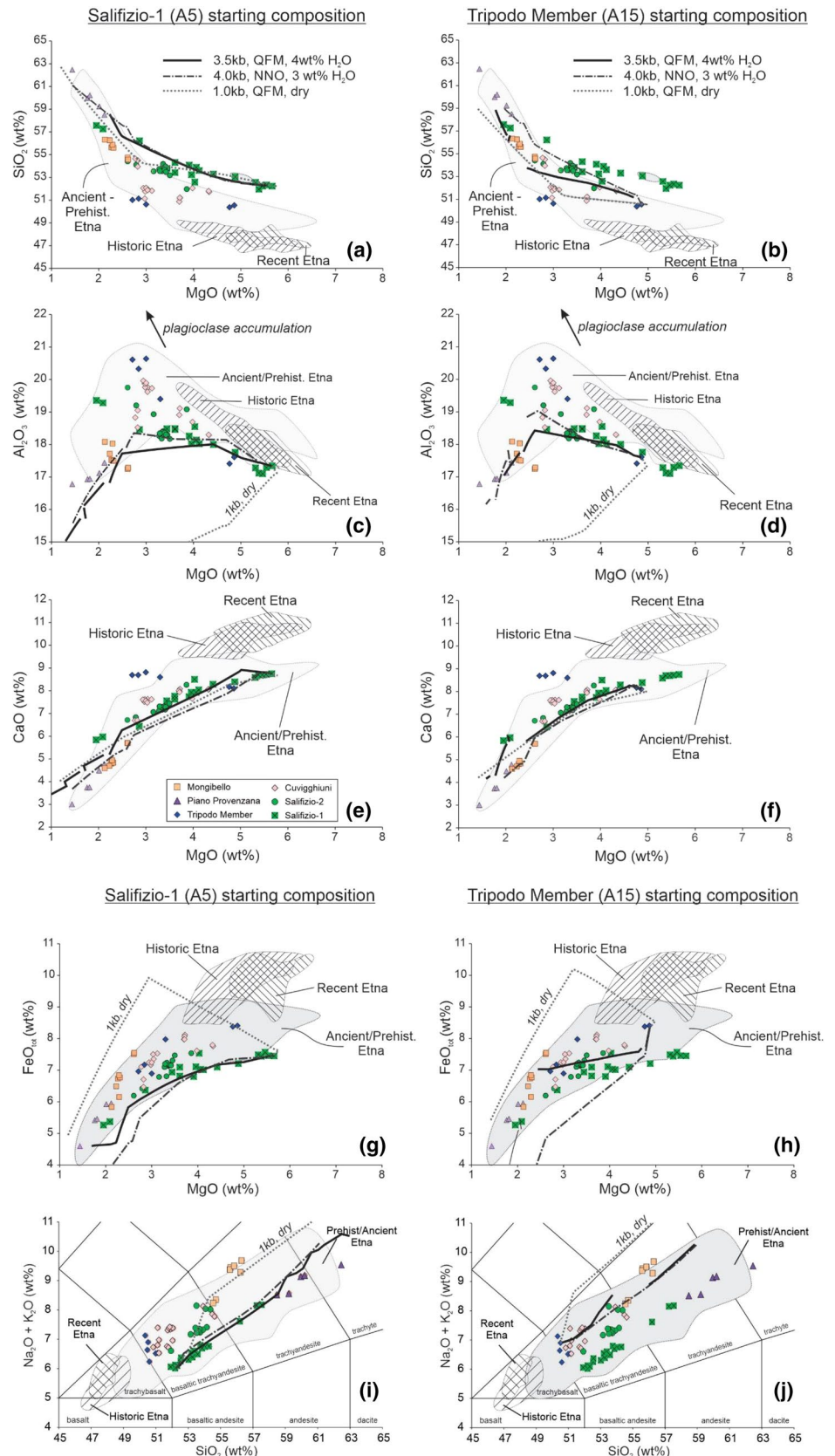
recent Etna in which the fractionation sequence is typically described as plagioclase, followed by clinopyroxene, olivine, titaniferous magnetite, and, in some cases, amphibole (Viccaro et al. 2011), all of which suggest a stronger imprint from shallower fractional crystallisation processes. Water concentrations of 3–4 wt% are consistent with the compositions of melt inclusions in olivine (Spilliaert et al. 2006), studies of Etna magma ascent rates (Armienti et al. 2013), and thermodynamic modelling (Kahl et al. 2015). Low values of loss on ignition (Table 2) suggest the Valle del Bove lavas were thoroughly degassed before eruption.

Source components of Etna magmatism: evidence from major and trace elements

Fractional crystallisation has clearly affected the compositions of the Valle del Bove lavas (Figs. 2, 3, 7). Nonetheless, some of the major and trace element variations observed may be an indication of differences in mantle source composition or variations in percentage of melting, rather than differences in extent of fractionation.

We test this hypothesis using Th, a highly incompatible trace element, as a proxy for alkaline magma fractionation (Wilson et al. 1995) (Fig. 8). Thorium correlates positively with Differentiation Index in the Valle del Bove suite ($R^2 = 0.75$), further justifying this trace element approach (see Online Resources 1, Fig. S3). In the absence of significant crustal contamination, the ratio of two highly incompatible elements (i.e., $D \ll 1$) should remain largely unchanged during fractional crystallisation. Therefore, plots of Th versus other highly incompatible trace elements should produce linear arrays that project back to the ratio of the two elements in the parental magma, providing an indication of source composition and possible heterogeneity (e.g., Allegre et al. 1977; Joron and Treuil 1989). Given that the Valle del Bove lavas are characterised by an anhydrous phenocryst assemblage consisting of clinopyroxene + plagioclase + magnetite ± olivine (Spence and Downes 2011), elements such as Nb, Zr, and Ba should have similar incompatibility during fractional crystallisation in this system (see GERM database, https://earthref.org/KDD/). Figure 8a shows that most Valle del Bove lavas overlap the field of prehistoric/ancient Etna and form arrays with Nb/Th ratios similar to recent and historic Etna. Some lavas from Salifizio-1, however, appear to have evolved from a parental magma that was more enriched in Th relative to Nb. Moreover, if the Piano Provenzana lavas evolved from a transitional/silica-saturated parent similar to Salifizio-1, as suggested by Fig. 2 and S2, these lavas are significantly more enriched in Nb (or depleted in Th) than expected by fractional crystallisation alone. In the plots of Ba and Zr vs Th (Fig. 8b, c), the Valle del Bove samples again largely overlap the field for prehistoric/ancient Etna, but the slopes of the data at the highest
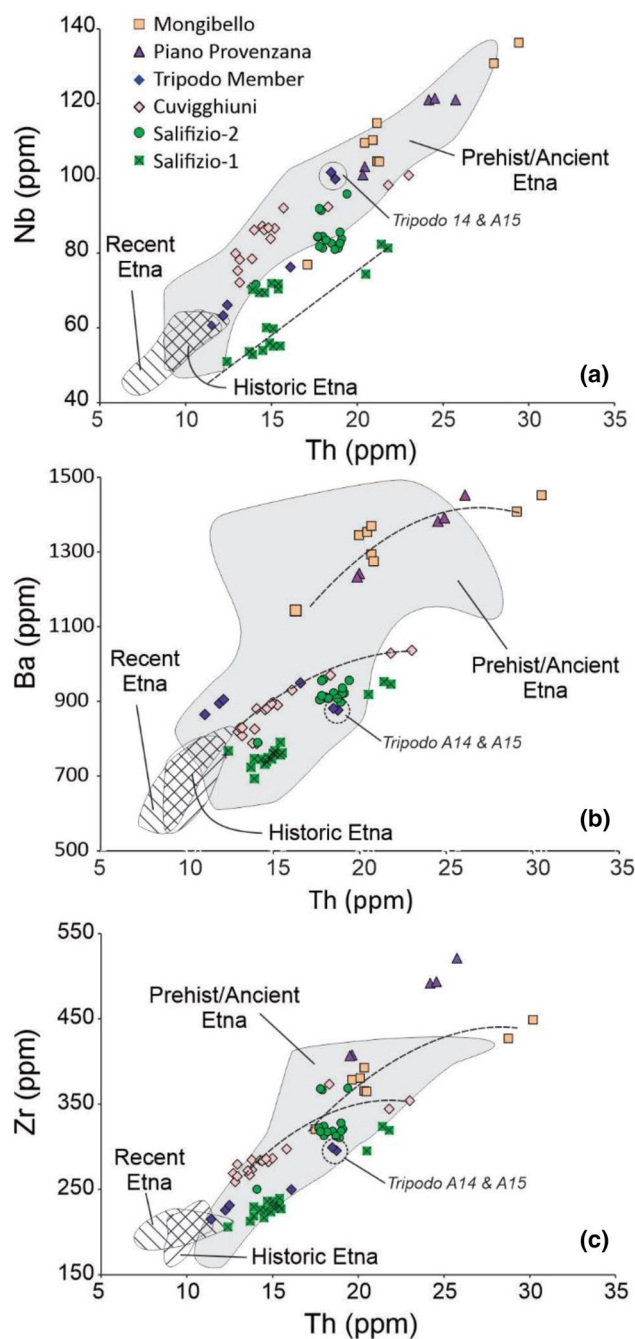

Fig. 8 **a** Nb versus Th, **b** Ba versus Th, and **c** Zr versus Th concentrations. Thorium is used as a proxy for alkaline magma fractionation of the six Valle del Bove units. Data sources for ancient to recent Etna magmatism as in Fig. 3

degrees of fractionation are shallower than expected within individual units; that is, at the highest Th concentrations (i.e., highest fractionation), Ba and Zr concentrations are lower than expected. Instead, the data are better described by second–order polynomials ($R^2 > 0.86$), as shown in Fig. 8b, c. At lower Th concentrations (lower fractionation), the curves indicate similar Ba/Th and Zr/Th ratios for recent

and historic Etna, but as magma differentiation increases, they deviate to lower Ba/Th and Zr/Th. This could be due to fractionation of trace phases with higher *D* values for these elements that appear later in the fractionation sequence, such as amphibole, biotite, or K-feldspar (for Ba), and zircon (for Zr). Nonetheless, as for Nb vs. Th, lavas from Salifizio-1 appear to have evolved from a parent that was enriched in Th relative to Ba and Zr, and the Piano Provenzana lavas have higher concentrations of Ba and Zr relative to Th than would be expected if they were derived from a silica-saturated parent similar to Salifizio-1. In addition, the two least evolved Tripodo member samples, A14 and A15 (MgO > 4.75 wt%; samples circled in Fig. 8a–c), clearly have higher concentrations of incompatible trace elements than the more evolved lavas from this unit (MgO < 3.3 wt%), opposite to what would be expected if the rocks were related by fractional crystallisation.

The data, therefore, demonstrate that at least some of the trace element variations observed are unrelated to fractional crystallisation (Fig. 8). These findings further suggest that crustal contamination is unlikely to be responsible for the trace element variations, since average continental crust (Rudnick and Gao 2003) has concentrations of Nb (8 ppm), Zr (132 ppm), Ba (456 ppm), and Th (6 ppm) that are lower than those in the least evolved Valle del Bove samples. This conclusion is consistent with similar trace element arguments against significant crustal assimilation put forward for recent Etna by Corsaro et al. (2007). In addition, D'Orazio et al. (1997) observed Sr and Nd isotope equilibrium between clinopyroxene and host lavas from the north wall of the Valle del Bove, which indicates that if crustal contamination occurred, it could not have taken place after clinopyroxene began to crystallise. Similar evidence for phenocryst-melt isotopic equilibrium was also reported by Miller et al. (2017) for the older Timpe lavas. As shown by our alphaMELTS 1.9 modelling, crystallisation of clinopyroxene occurs very early in the fractionation sequence at moderate pressures, thus limiting the potential for impact from shallow-level crustal contamination.

Despite the similarities in incompatible element ratios and, hence, potential source regions for recent to ancient Etna as suggested by Fig. 8, Fig. 4b shows that even the most primitive of the Valle del Bove samples, i.e., some samples from Salifizio-1 and the Tripodo member, are enriched in Ba, Th, Nb, Pb, and Zr relative to recent and historic Etna magmas. Furthermore, these two units are not only distinct from recent and historic Etna, but also different from one another, suggesting differences in source composition or petrogenesis. The Tripodo member has a trace element pattern similar to average historic Etna lavas, just at higher overall concentrations, consistent with the lavas being slightly more evolved (Fig. 3). In contrast, Salifizio-1 lavas have higher Rb and Th, but lower light rare earth

elements (LREE) and Sr. Strong relative depletions in Sr indicate a role for plagioclase fractionation, and the trough at Ti reflects magnetite fractionation (Fig. 4b). The low K concentration would be consistent with fractionation of a K-bearing phase, such as biotite or K-feldspar, but neither of these phases is observed in the rocks. Instead, the relative depletion in K is more likely an indication of derivation from a source in which a K-bearing phase, such as phlogopite or amphibole, was residual during partial melting, as suggested by Viccaro and Cristofolini (2008) for recent Etna lavas.

This interpretation is consistent with our own modelling of K and Rb systematics for the Valle del Bove lavas (Fig. 9). In a plot of K/Rb ratio versus Rb concentration, the Valle del Bove samples overlap the fields for historic and recent Etna but extend to higher concentrations of Rb for a given K than seen in the younger Etna rocks, particularly for the highly evolved lavas from Piano Provenzana and Mongibello. The effects of clinopyroxene and amphibole fractionation are
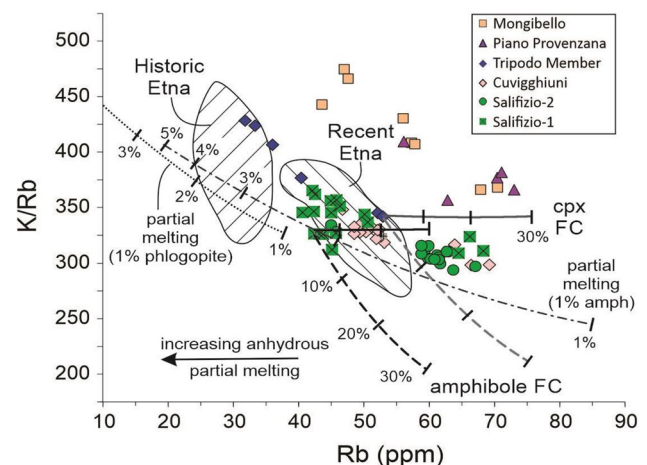

Fig. 9 K/Rb ratios versus Rb concentrations showing calculated trends for partial melting of a source containing 1 modal % phlogopite (dotted line) and 1 modal % amphibole (dot-dash line). Variations due to fractional crystallisation of amphibole from starting compositions A5 (Salifizio-1) and A15 (Tripodo member) shown as dashed lines. Variations due to fractional crystallisation of clinopyroxene from starting compositions A5 and A15 shown as solid lines. Data sources for ancient to recent Etna samples as in Fig. 3. Fractional crystallisation modelled using the equation $C_L = C_o * F^{(D-1)}$, where C_L is the calculated liquid composition, C_o is the initial concentration, D is the bulk distribution coefficient and F is the fraction of liquid remaining. Partial melting calculations assume simple batch melting, i.e., $C_L = C_o/(D + F - DF)$, where C_L is the calculated liquid composition, C_o is the initial concentration, D is the bulk distribution coefficient and F is the degree of partial melting. Mineral modes are based on anhydrous lherzolite xenoliths from the Iblean Plateau (ol = 72%; opx = 15%; cpx = 12%, Correale et al. 2014) modified to include 1% amphibole or 1% phlogopite. Partition coefficients from GERM (https://earthref.org/KDD/); Rb partition coefficients as follows: ol = 0.0003; opx = 0.001; cpx = 0.01; amph = 0.023; phlog = 1.5; K partition coefficients: ol = 0.0001; opx = 0.0003; cpx = 0.004; amph = 1.36; phlog = 3

shown as the solid and dashed lines, respectively. Fractionation in the absence of a hydrous phase would increase Rb concentrations but have little effect on the K/Rb ratio (solid lines). Because K is more compatible in amphibole than Rb, fractionation of this phase would decrease the K/Rb ratio while increasing the Rb concentration (dashed lines). While some of the Valle del Bove data are consistent with a small amount of amphibole fractionation, in most cases, our modelling suggests that fractionation is dominated by anhydrous phases, in support of our MELTS modelling (Fig. 7).

However, fractionation of the observed phenocryst phases cannot account for the lower Rb and higher K/Rb values of some Tripodo or Mongibello samples, assuming parental magma compositions like those of the most primitive lavas in the suite. Indeed, the most primitive lavas, e.g., A5 from Salifizio-1 and A15 from the Tripodo member, overlap the field of recent Etna, whereas the more evolved samples from the Tripodo member overlap the field for historic Etna, and evolved rocks from Mongibello have both higher K/Rb ratios and Rb concentrations (Fig. 9). These differences suggest either different source compositions or differences in the degree of melting that gave rise to the parental magma, or both.

We evaluate these two alternatives via a simple batch partial melting model of a spinel lherzolite source containing either 1% amphibole or 1% phlogopite in the mode (Fig. 9). The two curves have similar shapes and show similar trajectories of increasing K/Rb ratios with decreasing Rb concentration as degree of partial melting increases, similar to the distribution shown by the Etna data. The phlogopite-bearing source, however, produces lower concentrations of Rb and higher K/Rb ratios for the same degree of partial melting relative to the amphibole-bearing source. More sophisticated melting models, such as non-modal batch melting or fractional melting, tend to produce higher Rb concentrations and K/Rb ratios for smaller degrees of partial melting. In contrast, partial melting of an anhydrous peridotite source would produce a nearly horizontal array on this diagram given the similar partition coefficients for the relevant mineral phases.

Collectively, the data suggest that the Etna lavas were derived by partial melting of a source containing hydrous phases, such as amphibole or phlogopite. The trend of increasing K/Rb ratios with decreasing Rb concentration as a function of degree of partial melting is more consistent with the observed data distribution than melting of an anhydrous source. The offset of the Tripodo member samples and historic Etna to lower Rb and higher K/Rb relative to recent Etna suggests these magmas were either derived by larger degrees of partial melting or from a different source.

The modelling results in Fig. 9 do not allow unambiguous distinction between these two options, because details of source mineralogy and elemental concentrations can only

be assumed. However, several lines of evidence lead us to conclude that the Tripodo member lavas were derived by smaller degrees of partial melting than the Salifizio-1 lavas, e.g., their more silica undersaturated compositions (Fig. 2 and S1), higher La/Y, and lower Rb, Th, and K relative to Ba, Nb, and La (Fig. 4). Therefore, source heterogeneity has likely played a significant role in generating the compositional variations observed.

Source components of Etna magmatism: evidence from Sr:Nd:Pb:Hf isotopes

Many authors have interpreted the compositional variations in recent Etna lavas as evidence for source heterogeneity (e.g., Carter and Civetta 1977; Tanguy et al. 1997; Tonarini et al. 2001; Armienti et al. 2004; Viccaro and Cristofolini 2008; Viccaro et al. 2011; Correale et al. 2014 and references therein). Models to explain this source heterogeneity are broadly of two types. One calls for modification of the mantle source via subduction-derived melts and fluids, a model consistent with the complex geodynamic setting in which Etna is located (e.g., Armienti et al. 2004; Tonarini et al. 2001; Viccaro et al. 2011). The other attributes source heterogeneity to lithologic variations in which a predominantly lherzolitic matrix is crosscut by pyroxenite ($\pm$ garnet) veins (Correale et al. 2014; Miller et al. 2017; Viccaro and Zuccarello 2017). Correale et al. (2014) further argue that the pyroxenitic component contributes about 10% to the melts that give rise to recent Etnean lavas.

Constraining the proportion of pyroxenite to peridotite in the mantle source is challenging because (a) pyroxenite compositions can vary widely (Downes 2007; Lambart et al. 2016) and (b) phase relations, and hence melt compositions, are pressure and temperature sensitive. Nonetheless, in broad terms, partial melts involving high proportions of pyroxenite in the source tend to be higher in CaO/Al_2O_3 and TiO_2 but lower in SiO_2 for a given MgO concentration than those derived from peridotite melting (Kogiso et al. 2003; Condamine and Medard 2016). Thus, the higher SiO_2, lower CaO/Al_2O_3, FeO, and TiO_2 of prehistoric Etna magmas relative to recent and historic Etna (Fig. 3) are consistent with an increase in the proportion of pyroxenite in the source of Etna magmas over time.

Variations in isotopic composition also allow us to examine source heterogeneity and to assess several different processes that may be involved in the petrogenesis of the Valle del Bove lavas: (1) melting of isotopically distinct asthenospheric mantle sources; (2) variable degrees of partial melting of metasomatised mantle domains; (3) addition of a subduction-related component to the mantle source; and (4) crustal contamination of magmas during fractionation. In the following sections we consider the relative contributions of these various processes.

Recent and historic Etnean lavas are generally considered to have been derived from an asthenospheric mantle source (Wilson and Downes 2006), known variously as the low-velocity composition (LVC) of Hoernle et al. (1995), the European asthenospheric reservoir (EAR) of Cebrià and Wilson (1995), the common component ('C') of Hanan and Graham (1996), or the FOcal ZOne (FOZO) of Hart et al. (1992). This mantle component may itself be a mixture, with contributions from DMM (low ^{87}Sr/^{86}Sr and radiogenic (high) Nd, Hf, and Pb isotopic compositions) and possibly EM1 sources (enriched mantle-1) (Stracke et al. 2005; Viccaro et al. 2011). The isotopic compositions of the Iblean Plateau lavas (Figs. 5, 6) indicate an origin from a more depleted mantle source than that feeding present-day Mt. Etna (Tonarini et al. 1996; Trua et al. 1998). Hence, modern Etna is no longer tapping the depleted mantle source of the older Iblean tholeiitic magmatism. Instead, modern Etna is being fed by an isotopically heterogeneous mantle source more typical of intra-plate ocean islands (Armienti et al. 1989; Tonarini et al. 2001; Viccaro and Cristofolini 2008). Surprisingly, our study shows that Salifizio-1 lavas, the oldest lavas in our suite, have isotopic compositions similar to those of recently erupted Etna lavas, whereas, four slightly younger units (Salifizio-2, Cuvigghiuni, Tripodo, and Mongibello) have tapped a source very similar to that of historic Etna lavas (Fig. 5). In contrast, Piano Provenzana lavas show a unique isotopic signature that has not previously been recognised in the data for Mt. Etna. Although major and trace element data provide no evidence for significant involvement of crustal contamination in the petrogenesis of Valle del Bove lavas, we still need to consider this process with regard to the isotope data before we can confidently interpret this new isotopic signature as an indication of source heterogeneity.

Crustal contamination versus a subducted sediment component: evidence from Sr:Nd:Pb:Hf isotopes

The composition of the lower crust beneath NE Sicily is not well constrained, since the only crustal xenoliths available are derived from the upper crust and have experienced extensive thermal metamorphism (Michaud 1995). The outcropping basement NE of Mt. Etna is composed of a variety of metasedimentary rocks intruded by Hercynian granitoids (Fiannacca et al. 2008) and thus closely resembles the crust of the Calabrian arc and other areas of Hercynian crust throughout southern Europe, but there are few studies of the geochemistry and isotopic compositions of these rocks. We have therefore used Sr, Nd, and Pb isotopic data for metaigneous and metasedimentary lower crustal xenoliths from the Hercynian French Massif Central (Downes et al. 1990) as proxies in concert with the limited information available on Calabrian basement

(Caggianelli et al. 1991; Rottura et al. 1991). The average Hf isotope composition of the same Hercynian lower crustal xenoliths (Vervoort et al. 2000) has been used here as a proxy for the crust underneath Mt. Etna.

Lead isotope data for the Valle del Bove lavas show a tightly constrained linear array in comparison to circum-Tyrrhenian volcanic rocks (Fig. 10). Most samples plot within or near the FOZO/EAR/LVC/C field with high ^{206}Pb/^{204}Pb ratios, while the Piano Provenzana lavas have lower ^{206}Pb/^{204}Pb and trend towards the general fields of sediments or continental crust. The solid black arrows in Fig. 10a, b indicate possible mixing trajectories that could explain the Valle del Bove Pb isotope arrays. The data are inconsistent with assimilation of Hercynian-type upper continental crust, but could be explained by incorporation of subducted sediment like that seen in the eastern Mediterranean (Klaver et al. 2015) or Ionian Sea (Kempton et al. 2018) into a FOZO/EAR-type source. Assimilation of Calabrian-type basement is also consistent with the Pb isotope data, and we cannot distinguish these alternatives using Pb isotope data alone.

However, Calabrian basement has an average ^{87}Sr/^{86}Sr value of ca. 0.717 (Caggianelli et al. 1991; Rottura et al. 1991), so assimilation-fractional crystallisation processes involving such a contaminant would likely have also affected ^{87}Sr/^{86}Sr, which is not observed (Fig. 5). Furthermore, all analysed Etna lavas have > 700 ppm Sr (compared to < 250 ppm for Calabrian basement), so it is unlikely that assimilation of continental crust would strongly affect their Sr isotope compositions. Nevertheless, the Piano Provenzana lavas clearly provide evidence for the presence of a component with a lower ε_{Hf} and ε_{Nd} composition beneath Etna (Fig. 5d, f).

The uniqueness of this component is particularly apparent in comparisons of the Valle del Bove units in ^{176}Hf/^{177}Hf vs ^{206}Pb/^{204}Pb in the context of the wider regional data set (Fig. 11a). Most of the Valle del Bove lavas again show a well-constrained array with one end–member in the FOZO/EAR field; the data partially overlap the field for recent and historic Etna, but are clearly distinct from the sources of the Iblean Plateau and Aeolian arc (Alicudi and Filicudi), the compositions of which indicate greater time-integrated incompatible element depletion. Paired Hf–Pb isotopic data for other prehistoric Etna rocks are limited, but four analyses from the Timpe Santa Caterina phase of activity, i.e., 220–100 ka (Miller et al. 2017), have high Hf isotope values that overlap the composition of the Iblean Plateau. The Pb isotope compositions of these rocks are, however, more HIMU-like than those from the Iblean Plateau and, instead, are similar to the most radiogenic lavas from Valle del Bove. Thus, based on currently available data, the low Hf isotope values of the Piano Provenzana lavas are unlike any known Etna magmatic products.

Fig. 10 a ^{207}Pb/^{204}Pb versus ^{206}Pb/^{204}Pb and **b** ^{208}Pb/^{204}Pb versus ^{206}Pb/^{204}Pb ratios for volcanic rocks of the circum-Tyrrhenian area. Calculated trend line indicates potential mixing of FOZO/EAR/LVC/C source components with a crustal or sedimentary component. Data sources as in Fig. 6 with additional data from Ayuso et al. (1998), Barnekow (2000), Beccaluva et al. (1990), Belkin and De Vivo (1993), Calanchi et al. (2002), Civetta et al. (1981, 1998), Conticelli and Peccerillo (1992), Conticelli (1998), Conticelli et al. (2009), Crisci et al. (1991), D'Antonio and Di Girolamo (1994), D'Antonio et al. (1996, 1999), DeAstis et al. (2000, 2006), Del Moro et al. (1998), Di Renzo et al. (2007), Downes et al. (2001), Ellam et al. (1989), Esperança et al. (1992), Esperança and Crisci (1995), Francalanci et al. (1993), Gertisser and Keller (2000), Gioncada et al. (2003), Kempton et al. (2018), Orsi et al. (1995), Pappalardo et al. (2002), Peccerillo (1992), Perini et al. (2004), Pinarelli (1991), Prosperini (1993), Santo et al. (2004), and Vollmer (1976). Fields for average Hercynian lower and upper continental crust from Downes et al. (1990, 1991, 1997). Field for Mediterranean sediment samples from Klaver et al. (2015) and Kempton et al. (2018). *EAR* European Asthenospheric Reservoir (Cebrià and Wilson 1995); *LVC* low velocity composition (Hoernle et al. 1995), *FOZO* FOcal ZOne (Hart et al. 1992), *'C'* common component (Hanan and Graham 1996), *NHRL* Northern Hemisphere Reference Line (Hart 1984)
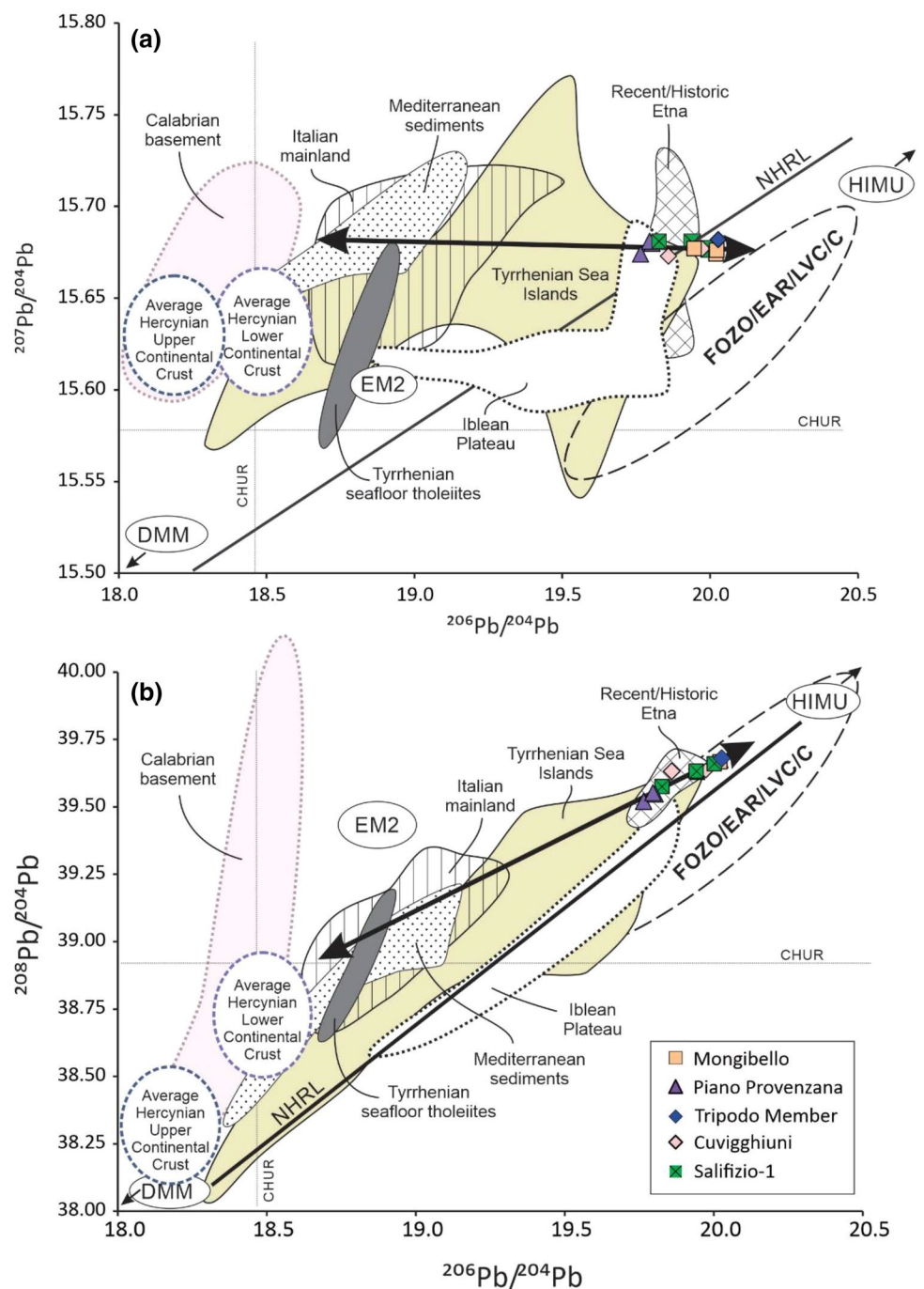
Piano Provenzana: a new component in Etna magmatism?

Figures 5 and 11 indicate that the lavas from Piano Provenzana are isotopically unique among Etna magmatic products. One interpretation is that a brief episode of melting of an unusual sediment component in the slab beneath Sicily may have given rise to the source of the Piano Provenzana lavas. Comparisons of ^{176}Hf/^{177}Hf and Nd/Zr (Fig. 12a) show that all the prehistoric lavas analysed in this study have lower Nd/

Zr than recent or historic Etna, while only the Piano Provenzana lavas have Hf isotope compositions lower than recent and historic Etna. Thus, the lower Hf isotope signature in the Piano Provenzana unit might be related to zircon-rich sediments introduced into the mantle wedge prior to mixing with an upwelling melt generated from a more depleted mantle end–member, i.e., the "zircon effect" (Patchett et al. 1984; White et al. 1986; Blichert-Toft et al. 1999; Carpentier et al. 2009). Mixing calculations (Fig. 11b) show that isotopic signatures of most Valle del Bove samples can be
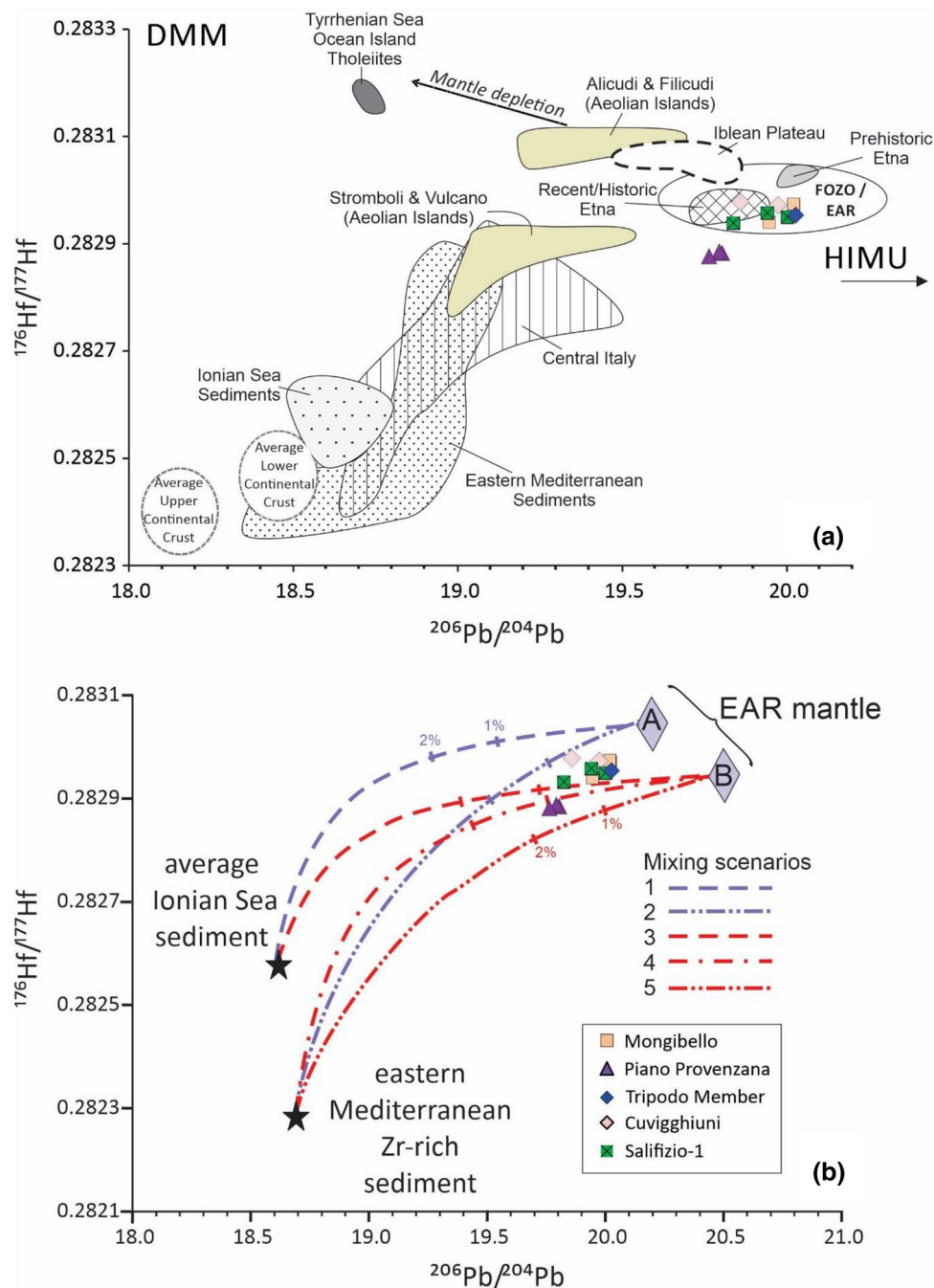
Fig. 11 a $^{176}Hf/^{177}Hf$ versus $^{206}Pb/^{204}Pb$ ratios for Valle del Bove samples in the context of the wider data set for Italian/Tyrrhenian volcanic rocks and the field for LVC/EAR/FOZO/C field. Data sources as for Figs. 5 and 10 with additional Hf isotopic data for Italy and the Tyrrhenian Sea from Barnekow (2000), Conticelli and Peccerillo (1992), Prelević et al. (2010), and Miller et al. (2017). Average Hf isotopic composition for Hercynian lower and upper continental crust from Vervoort et al. (1999, 2000). Mediterranean sediment data from Klaver et al. (2015) and Kempton et al. (2018). **b** Five representative mixing scenarios between EAR-type mantle and possible subducted sediment calculated using IgPet (Carr and Gazel 2017). EAR mantle modelled using two compositions: EAR **a** is representative of prehistoric Etna from Timpe Santa Catalina (Miller et al. 2017), i.e., $^{176}Hf/^{177}Hf = 0.28305$; $^{206}Pb/^{204}Pb = 20.2$; EAR **b** is more HIMU-like and more typical of the most enriched Valle del Bove lavas, i.e., $^{176}Hf/^{177}Hf = 0.28295$; $^{206}Pb/^{204}Pb = 20.5$; Hf and Pb concentrations in both cases assume primitive mantle values of 0.309 and 0.185 ppm, respectively (Sun and McDonough 1989). Average Ionian sediment from Kempton et al. (2018): $^{176}Hf/^{177}Hf = 0.28229$; $^{206}Pb/^{204}Pb = 18.7$; Hf = 2.6 ppm; Pb = 12.3 ppm. Eastern Mediterranean Zr-rich sediment from Klaver et al. (2015): $^{176}Hf/^{177}Hf = 0.28258$; $^{206}Pb/^{204}Pb = 18.6$; Hf = 3.2 ppm; Pb = 12.5 ppm. Tick marks on the mixing curves represent 1% and 2% mixing of the sediment component into the EAR mantle source; further percentages of mixing omitted from the figure for clarity
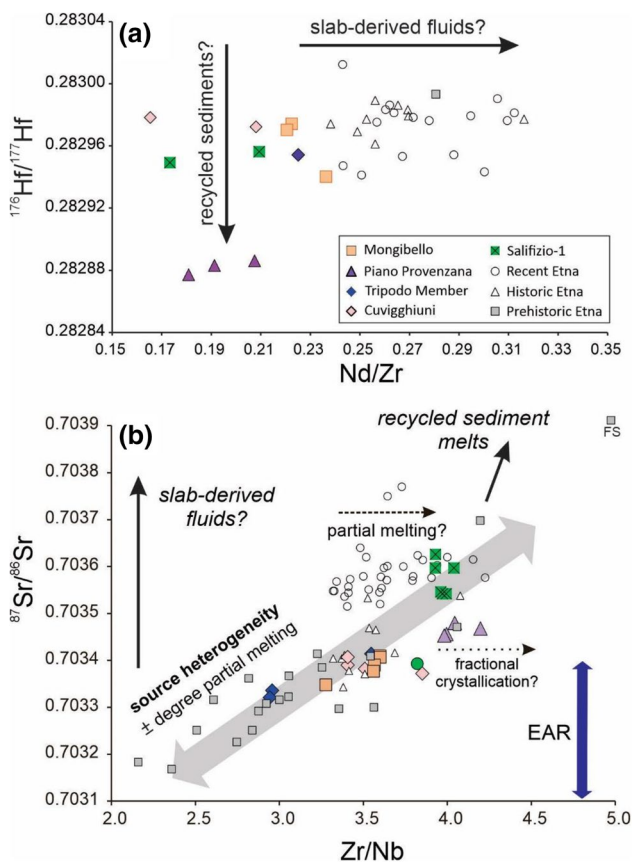
Fig. 12 **a** ^{176}Hf/^{177}Hf versus Nd/Zr ratios for the six Valle del Bove units, recent Etna, and historic Etna. Adapted from a diagram by Nicotra et al. (2013). **b** ^{87}Sr/^{86}Sr versus Zr/Nb ratios for the six Valle del Bove units compared with the data fields for recent, historic, and ancient/prehistoric Etna; prehistoric Etna sample labelled FS is the unusual picrite reported by Correale et al. (2014). Solid black arrows indicate direction of compositional variation from slab-derived fluids and/or recycled sediment melts. Dashed arrow indicates compositional variation for recent Etna as a result of partial melting as proposed by Viccaro and Cristofolini (2008); dotted arrow indicates variation as a result of fractional crystallisation for most evolved VdB compositions where there is potential to fractionate Zr/Nb through crystallisation of phases like titanomagnetite or sphene. EAR compositional range (double-headed arrow) from Cebrià and Wilson (1995). Data sources as in Fig. 5

explained by incorporation into a FOZO/EAR-type mantle source of < 2 wt% sediment similar in composition to that of the Ionian Sea (Kempton et al. 2018). The Piano Provenzana samples, however, require a sediment contaminant with a lower Hf isotope composition, such as the Zr-rich sediments of the eastern Mediterranean (Klaver et al. 2015). A similar model was used recently to explain the Hf–Nd isotope systematics of Miocene subduction-related rocks from Sardinia (Kempton et al. 2018).

However, if a subduction component is involved in the mantle source of the Piano Provenzana lavas, this addition must have occurred prior to 42–30 ka, the age of the Piano

Provenzana lavas according to De Beni et al. (2011). Moreover, ^{87}Sr/^{86}Sr appears to have been largely unaffected by this process relative to other lavas of Ellittico. The Tripodo member, for example, comprises low-SiO$_2$ lavas with an age range similar to that of the upper Piano Provenzana formation (Branca et al. 2011a; De Beni et al. 2011), and these lavas exhibit low ^{87}Sr/^{86}Sr and high ^{176}Hf/^{177}Hf (Fig. 5). Furthermore, the degree of isotopic offset of the Piano Provenzana lavas from other prehistoric Etna lavas (Figs. 5, 6, 12) decreases in the order: Hf > Nd > Pb > Sr. In other words, the fluid-immobile elements Hf and Nd show a greater offset than the fluid-mobile elements Pb and Sr.

Thus, the lower ^{176}Hf/^{177}Hf values (relative to all other Etna lavas) could imply melting of an additional (ancient?) component in the source of the Piano Provenzana lavas, rather than recent fluid transfer during subduction. The unique isotope composition is consistent with small-scale heterogeneity in the form of veins or metasomatic minerals in the mantle source, i.e., mantle metasomes. Such a process has been described from numerous localities worldwide in which low-degree melts, enriched in highly incompatible elements, ascend and undergo fractional crystallisation, producing a spectrum of mineral assemblages ranging from anhydrous veins (chiefly pyroxenites ± garnet) to hydrous cumulates that contain amphibole and phlogopite (e.g., Frey and Prinz 1978; Irving 1980; Kempton 1987; Bodinier et al. 1990; Harte et al. 1993; Downes 2007). Viccaro and Zuccarello (2017) recently showed that partial melting of a mixed peridotite-pyroxenite mantle source could produce alkaline compositions similar to those of recent Etna magmas. In their model the peridotite component is a spinel lherzolite that contains hydrous metasomatic phases, whereas, the pyroxenite component is a garnet pyroxenite formed by crystallisation of silicate melts. They concluded that the pyroxenite to lherzolite ratio required to explain the compositions of recent Etna lavas ranges from 10 to 35%.

This model is consistent with the Valle del Bove data as shown in Fig. 12b, a plot of ^{87}Sr/^{86}Sr vs. Zr/Nb. Zr and Nb are relatively immobile in fluids mobilised during subduction, and since both are moderately incompatible, variation in the Zr/Nb ratio as a function of partial melting of a homogeneous source should be relatively small. Isotope ratios are obviously not fractionated during mantle melting, so any variation observed is a function of source heterogeneity. The data show a broad correlation between ^{87}Sr/^{86}Sr and Zr/Nb for ancient Etna and most Valle del Bove lavas. Historic and recent Etna lavas plot at the high-Zr/Nb end of the array, although recent Etna lavas have consistently higher ^{87}Sr/^{86}Sr for a given Zr/Nb relative to older lavas. If modification of the mantle source via subduction-derived fluids was the primary control on isotopic and trace element variations, there should be no obvious correlation between Zr/Nb and ^{87}Sr/^{86}Sr.

It could be argued that the trend is due to a fortuitous combination of subduction enrichment, which produces a vertical trend on the diagram through addition of radiogenic Sr, plus variation in Zr/Nb as a function of degree of partial melting induced by that fluid addition. This scenario implies that the degree of subduction modification correlates systematically with the degree of partial melting of the metasomatised mantle. However, the difference in degree of partial melting required to create the observed range of Zr/Nb ratios is at least a factor of 10, which would have a significant impact on the major element compositions of the magmas produced. In such a scenario, the lowest Zr/Nb should be significantly more enriched in other incompatible trace elements and probably more silica undersaturated than those at the high Zr/Nb end of the array, and such systematic variation is not observed for the data set as a whole (see Online Resources 1, Fig. S4). While we cannot entirely rule out this scenario, the impact from garnet pyroxenite in the source, which has a Zr/Nb of > 25 based on data for Iblean ultramafic xenoliths (Correale et al. 2012), is likely to outweigh the impact of varying degrees of partial melting of a homogeneous lherzolitic source, which typically has a Zr/Nb ratio < 4. As such, the broad positive correlation is more likely due to a heterogeneous source consisting of variable proportions of lherzolite and pyroxenite.

This suggests there is a compositional, i.e., source heterogeneity, control involved in the genesis of Etna magmas, particularly ancient and prehistoric Etna. Melts derived from a pyroxenite-rich source should have higher Zr/Nb than those from a lherzolitic source. The positive correlation between Sr isotopes and Zr/Nb, therefore, suggests a role for ancient veins in the mantle rather than recent subduction influences. On the other hand, the offset of recent Etna lavas to higher ^{87}Sr/^{86}Sr may reflect a more significant role for metasomatism of the mantle source via subduction-derived fluids for these rocks.

We therefore agree with the interpretations of Viccaro and Cristofolini (2008), Correale et al. (2014), Miller et al. (2017), and Viccaro and Zuccarello (2017) that the mantle beneath Etna is heterogeneous, consisting of a lherzolite matrix crosscut by streaks or veins of 'ancient' pyroxenite of variable composition. More recent modification by subduction-derived fluids and/or melts may contribute to the petrogenesis of historic and recent Etna magmas.

The isotopic variation seen in the prehistoric lavas from Mt. Etna may be related to a decreasing degree of mantle melting relative to that producing Iblean tholeiites, so that less depleted low-T melting components of the heterogeneous mantle are preferentially tapped (Conticelli et al. 1997; Pilet et al. 2011; Correale et al. 2014). In this scenario, the LREE and large-ion lithophile element (LILE) component of these rocks is likely to be related to decompression melting of a fusible part of the fluid-metasomatised upper mantle enriched with pyroxenites and/or hydrated minerals such as phlogopite or amphibole, as found in mantle xenoliths from the Iblean Plateau (Tonarini et al. 1996; Scribano et al. 2009; Bianchini et al. 2010). The Piano Provenzana parental melt may have formed in a discrete metasomatic zone in the mantle with an enriched crust-like signature (Downes 2007), i.e., veins with a lower Hf isotopic composition than the surrounding mantle but similar Sr isotopic composition, thus affecting the isotope composition of Hf more than that of Nd and Pb, and with little effect on ^{87}Sr/^{86}Sr.

Summary and conclusions

1. Analysed Valle del Bove samples represent six lithostratigraphic units of prehistoric Etna lavas ranging in age from ~ 85 to ~ 4 ka. They show differences in element and radiogenic isotopic compositions that vary between the signatures of recent and historic Etna samples, suggesting melting of two main mantle components in the asthenospheric mantle source over the past ~ 100 kyr.

2. Although, in broad terms, the source of magmatism in the region has changed over time from more DMM-like (for Iblean Plateau lavas) to a more enriched (FOZO/EAR/LVC/C-like) end–member for Etnean magmatism, variations in Sr:Nd:Pb:Hf isotopic compositions do not support a smooth transition. Instead, some of the oldest rocks for which data are available, e.g., Rocca Capra (~80 ka; D'Orazio et al. 1997) and Salifizio 1 (> 86 ka), encompass almost the entire range in Sr and Nd isotope values for Etna (0.70317 and 0.51293 for Rocca Capra, 0.70363 and 0.51283 for Salifizio-1).

3. Most of the prehistoric Etna eruptions tapped the FOZO/EAR/LVC/C asthenospheric mantle component. In contrast, evolved trachyandesites from the Piano Provenzana unit were derived from a source that is unique amongst analysed lavas from Mt. Etna, having a less radiogenic Hf isotope signature.

4. The low ^{176}Hf/^{177}Hf ratios of the Piano Provenzana lavas suggest they formed by melting of an unusual piece of metasomatised lithospheric mantle. Indeed, the data for Valle del Bove as a whole support the existence of a heterogeneous marble-cake-style mantle source variably metasomatized by hydrous phases (amphibole and/or phlogopite) and pyroxenite veins as suggested by several previous studies (Viccaro and Cristofolini 2008; Correalle et al. 2014; Miller et al. 2017; Viccaro and Zuccarello 2017). The proportion of pyroxenite appears to be greater in historic to recent Etna than in the Valle del Bove.

5. The degree of magmatic differentiation of Valle del Bove lavas is similar to that of recent and historic Etna,

but parental magmas were different and those for recent Etna were more silica undersaturated. Differences may be a function of degree of partial melting but are more likely due to different source compositions and, particularly, different proportions of pyroxenite in the source.

6. MELTS modelling, together with isotopic and trace element data, suggest that the Valle del Bove parental magmas contained ~ 3–4 wt% H_2O and fractionated in a magma chamber at moderate depths of ~ 10–12 km.

References

Albarède F, Télouk P, Blichert-Toft J, Boyet M, Agranier A, Nelson BK (2004) Precise and accurate isotopic measurements using multiple-collector ICPMS. Geochim Cosmochim Acta 68:2725–2744

Allègre CJ, Treuil M, Minster J-F, Minster B, Albarède F (1977) Systematic use of trace element in igneous process. Contrib Mineral Petrol 60:57–75

Armienti P, Innocenti F, Petrini R, Pompilio M, Villari L (1989) Petrology and Sr–Nd isotope geochemistry of recent lavas from Mt. Etna: bearing on the volcano feeding system. J Volc Geotherm Res 39:315–327

Armienti P, Tonarini S, D'Orazio M, Innocenti F (2004) Genesis and evolution of Mt Etna alkaline lavas: petrological and Sr–Nd–B isotope constraints. Period Di Mineral 73:29–52

Armienti P, Perinelli C, Putirka KD (2013) A new model to estimate deep-level magma ascent rates, with applications to Mt. Etna (Sicily, Italy). J Petrol 54(4):795–813. https://doi.org/10.1093/petrology/egs085

Asimow PD, Ghiorso MS (1998) Algorithmic modifications extending MELTS to calculate subsolidus phase relations. Am Mineral 83:1127–1132

Ayuso RA, De Vivo B, Rolandi G, Seal RR II, Paone A (1998) Geochemical and isotopic (Nd–Pb–Sr–O) variations bearing on the genesis of volcanic rocks from Vesuvius, Italy. J Volc and Geotherm Res 82:53–78

Barnekow P (2000) Volcanic rocks from central Italy: an Oxygen isotopic microanalytical and geochemical study. Ph.D. Thesis, University of Gottingen

Beccaluva L, Bonatti E, Dupuy C, Ferrara G, Innocenti F, Lucchini F, Macera P, Petrini R, Rossi PL, Serri G, Seyler M, and Siena F (1990) Geochemistry and mineralogy of volcanic rocks from ODP sites 650, 651, 655 and 654 in the Tyrrhenian Sea. In: Stewart NJ (ed) Proc Ocean Drilling Prog, Science Results. U.S. Govt. Print. Office Washington D.C., pp 49–73

Belkin HE, De Vivo B (1993) Fluid inclusion studies of ejected nodules from plinian eruptions of Mt. Somma-Vesuvius. J Volcanol Geotherm Res 58:98–100

Bianchini G, Yoshikawa M, Sapienza GT (2010) Comparative study of ultramafic xenoliths and associated lavas from South-Eastern Sicily: nature of the lithospheric mantle and insights on magma genesis. Mineral Petrol 98:111–121

Blichert-Toft J, Albarède F (1997) The Lu-Hf isotope geochemistry of chondrites and the evolution of the mantle-crust system. Earth Planet Sci Lett 148:243–258

Blichert-Toft J, Albarède F (2009) Mixing of isotopic heterogeneities in the Mauna Kea plume conduit. Earth Planet Sci Lett 282:190–200

Blichert-Toft J, Chauvel C, Albarède F (1997) Separation of Hf and Lu for high-precision isotope analysis of rock samples by magnetic sector-multiple collector ICP-MS. Contrib Mineral Petrol 127:248–260

Blichert-Toft J, Frey FA, Albarède F (1999) Hf isotope evidence for pelagic sediments in the source of Hawaiian basalts. Science 285:879–882

Bodinier JL, Vasseur G, Vernieres J, Dupuy C, Fabries J (1990) Mechanisms of mantle metasomatism: geochemical evidence from the Lherz orogenic peridotite. J Petrol 31:597–628

Bouvier A, Vervoort JD, Patchett PJ (2008) The Lu-Hf and Sm-Nd isotopic composition of CHUR: constraints from unequilibrated chondrites and implications for the bulk composition of terrestrial planets. Earth Planet Sci Lett 273:48–57

Branca S, Coltelli M, De Beni E, Wijbrans J (2008) Geological evolution of Mount Etna volcano (Italy) from earliest products until the first central volcanism (between 500 and 100 ka ago) inferred from geochronological and stratigraphic data. Intl J Earth Sci (geol Rundsch) 97:135–152

Branca S, Coltelli M, Groppelli G (2011a) Geological evolution of a complex basaltic stratovolcano: Mount Etna, Italy. Ital J Geosci (boll Soc Geol It) 130:306–317

Branca S, Coltelli M, Groppelli G, Lentini F (2011b) Geological map of Etna volcano, 1:50,000. Ital J Geosci (boll Soc Geol It) 130:265–291

Bryce JG, DePaolo DJ (2004) Pb isotopic heterogeneity in basaltic phenocrysts. Geochim Cosmochim Acta 68:4453–4468

Caggianelli A, Del Moro A, Paglionico A, Piccarreta G, Pinarelli L, Rottura A (1991) Lower crustal granite genesis connected with chemical fractionation in the continental crust of Calabria (Southern Italy). Eur J Mineral 3:155–180

Calanchi N, Peccerillo A, Tranne C, Lucchini F, Rossi PM, Kempton P, Barbieri M, Wu TW (2002) Petrology and geochemistry of the Island of Panarea: implications for mantle evolution beneath the Aeolian island arc (Southern Tyrrhenian Sea, Italy). J Volcanol Geotherm Res 115:367–395

Calvari S, Groppelli G, Pasquarè G (1994) Preliminary geological data on the south-western wall of the Valle del Bove, Mt. Etna. Sicily Acta Vulcanol 5:15–30

Cannata A, Di Grazia G, Giuffrida M, Gresta S, Palano M, Sciotto M, Viccaro M, Zuccarello F (2018) Space-time evolution of magma storage and transfer at Mt. Etna volcano (Italy): The 2015–2016 reawakening of Voragine crater. Geochem Geophys Geosyst 19:471–495. https://doi.org/10.1002/2017GC007296

Carpentier M, Chauvel C, Maury RC, Mattielli N (2009) The "zircon effect" as recorded by the chemical and Hf isotopic compositions of Lesser Antilles forearc sediments. Earth Planet Sci Lett 287:86–99

Carr MJ, Gazel E (2017) Igpet software for modeling igneous processes: examples of application using the open educational version. Miner Petrol 111:283–289

Carter SR, Civetta L (1977) Genetic implications of the Isotope and Trace Element variations in the eastern Sicilian volcanics. Earth Planet Sci Lett 36:168–180

Cebrià JM, Wilson M (1995) Cenozoic mafic magmatism in Western/Central Europe: a common European asthenospheric reservoir. Terra Nova Abst Supp 7:162

Chester DK, Duncan AM, Guest JE, Kilburn CRJ (1985) Mount Etna. Stanford University Press, The anatomy of a volcano (**ISBN 0-8047-1308-4**)

Civetta L, Innocenti F, Manetti P, Peccerillo A, Poli G (1981) Geochemical characteristics of potassic volcanics from Mt. Ernici (Southern Latium, Italy). Contrib Mineral Petrol 78:37–47

Civetta L, D'Antonio M, Orsi G, Tilton GR (1998) The geochemistry of volcanic rocks from Pantelleria Island, Sicily Channel: petrogenesis and characteristics of the mantle source region. J Petrol 39:1453–1491

Clocchiatti R, Joron J-L, Treuil M (1988) The role of selective alkali contamination in the evolution of recent historic lavas of Mt. Etna J Volcanol Geotherm Res 34:241–249

Coltelli M, Del Carlo P, Pompilio M, Vezzoli L (2005) Explosive eruptions of a picrite: the 3930 BP subplinian eruption of Etna volcano (Italy). Geophys Res Lett 32:L23307. https://doi.org/10.1029/2005GL024271

Condamine P, Médard E (2016) Devidal J-L (2016) Experimental melting of phlogopite-peridotite in the garnet stability field. Contrib Mineral Petrol 171:95. https://doi.org/10.1007/s00410-016-1306-0

Conticelli S (1998) The effect of crustal contamination on ultrapotassic magmas with lamproitic affinity: mineralogical, geochemical and isotope data from the Torre Alfina lavas and xenoliths, Central Italy. Chem Geol 149:51–81

Conticelli S, Peccerillo A (1992) Petrology and geochemistry of potassic and ultrapotassic volcanism in Central Italy: petrogenesis and inferences on the evolution of the mantle sources. Lithos 28:221–240

Conticelli S, Francalanci L, Manetti P, Cioni R, Sbrana A (1997) Petrology and geochemistry of the ultrapotassic rocks from the Sabatini Volcanic District, central Italy: the role of evolutionary processes in the genesis of variably enriched alkaline magmas. J Volcanol Geotherm Res 75:107–136

Conticelli S, Marchionni S, Rosa D, Giordano G, Boari E, Avanzinelli R (2009) Shoshonite and sub-alkaline magmas from an ultrapotassic volcano: Sr–Nd–Pb isotope data on the Roccamonfina volcanic rocks, Roman Magmatic Province, Southern Italy. Contrib Mineral Petrol 157:41–63

Correale A, Martelli M, Paonita A, Rizzo A, Brusca L, Scribano V (2012) New evidence of mantle heterogeneity beneath the Hyblean Plateau (southeast Sicily, Italy) as inferred from noble gases and geochemistry of ultramafic xenoliths. Lithos 132–133:70–81

Correale A, Paonita A, Martelli M, Rizzo A, Rotolo SG, Corsaro RA, Di Renzo V (2014) A two-component mantle source feeding Mt. Etna magmatism: Insights from the geochemistry of primitive magmas. Lithos 184–187:243–258

Corsaro RA, Pompilio M (2004) Dynamics of magmas at Mount Etna. Geophys Monogr 143:91–110

Corsaro RA, Neri M, Pompilio M (2002) Paleo-environmental and volcano-tectonic evolution of the southeastern flank of Mt. Etna during the last 225 ka inferred from the volcanic succession of the 'Timpe', Acireale. Sicily J Volc Geotherm Res 113:289–306

Corsaro RA, Miraglia L, Pompilio M (2007) Petrologic evidence of a complex plumbing system feeding the July–August 2001 eruption of Mt. Etna, Sicily, Italy. Bull Volcanol 69:401–421

Crisci GM, De Rosa R, Esperança S, Mazzuoli R, Sonnino M (1991) Temporal evolution of a three-component system: the Island of Lipari (Aeolian Arc, southern Italy). Bull Volcanol 53:207–221

D'Antonio M, Di Girolamo P (1994) Petrological and geochemical study of mafic shoshonitic volcanics from Procida-Vivara and Ventotene islands (Campanian Region, South Italy). Acta Vulcanol 5:69–80

D'Antonio M, Tilton GR, Civetta L (1996) Petrogenesis of Italian alkaline lavas deduced from Pb–Sr–Nd isotope relationships. Isotopic Studies of Crust-Mantle Evolution. AGU Monogr 95:253–267

D'Antonio M, Civetta L, Di Girolamo P (1999) Mantle source heterogeneity in the Campanian Region (South Italy) as inferred from geochemical and isotopic features of mafic volcanic rocks with shoshonitic affinity. Mineral Petrol 67:163–192

D'Orazio M, Tonarini S, Innocenti F, Pompilio M (1997) Northern Valle del Bove volcanic succession (Mt. Etna, Sicily): petrography, geochemistry and Sr–Nd isotope data. Acta Vulcanol 9:73–86

De Astis G, Peccerillo A, Kempton PD, La Volpe L, Wu TW (2000) Transition from calc-alkaline to potassium-rich magmatism in subduction environments: geochemical and Sr, Nd, Pb isotopic constraints from the island of Vulcano (Aeolian arc). Contrib Mineral Petrol 139:684–703

De Astis G, Kempton PD, Peccerillo A, Wu TW (2006) Trace element and isotopic variations from Mt. Vulture to Campanian volcanoes: constraints for slab detachment and mantle inflow beneath southern Italy. Contrib Mineral Petrol 151:331–351

De Beni E, Branca S, Coltelli M, Groppelli G, Wijbrans JR (2011) ^{40}Ar/^{39}Ar isotopic dating of Etna volcanic succession. Ital J Geosci (boll Soc Geol It) 130:292–305

Del Moro A, Gioncada A, Pinarelli L, Sbrana A, Joron JL (1998) Sr, Nd, and Pb isotope evidence for open system evolution at Vulcano, Aeolian Arc, Italy. Lithos 43:81–106

Di Renzo V, Vito MA, Arienzo I, Carandente A, Civetta L, D'Antonio M, Giordano F, Orsi G, Tonarini S (2007) Magmatic history

of Somma-Vesuvius on the basis of new geochemical and isotopic data from a deep borehole (Camaldoli della Torre). J Petrol 48:753–784

Di Renzo V, Corsaro RA, Miraglia L, Pompilio M, Civetta L (2019) Long and short-term magma differentiation at Mt. Etna as revealed by Sr–Nd isotopes and geochemical data. Earth Sci Rev 190:112–130. https://doi.org/10.1016/j.earscirev.2018.12.008

Doglioni C, Innocenti F, Mariotti G (2001) Why Mt Etna? Terra Nova 13:25–31

Downes H (2007) The origin of spinel- and garnet-pyroxenites in the shallow lithospheric mantle. Lithos 99:1–24

Downes H, Dupuy C, Leyreloup AF (1990) Crustal evolution of the Hercynian belt of Western Europe: Evidence from lower-crustal granulitic xenoliths (French Massif Central). Chem Geol 83:209–231

Downes H, Kempton PD, Briot D, Harmon RS, Leyreloup AF (1991) Pb and O systematics in granulite facies xenoliths, French Massif Central: implications for crustal processes. Earth Planet Sci Lett 102:342–357

Downes H, Shaw A, Williamson BJ, Thirlwall MF (1997) Sr, Nd and Pb isotopes in Hercynian granodiorites and monzogranites, Massif Central, France. Chem Geol 136:99–122

Downes H, Thirlwall MF, Trayhorn SC (2001) Miocene subduction-related magmatism in southern Sardinia: Sr–Nd– and oxygen isotopic evidence for mantle source enrichment. J Volcanol Geotherm Res 106:1–21

Eisele J, Abouchami W, Galer SJG, Hofmann AW (2003) The 320 kyr Pb isotope evolution of Mauna Kea lavas recorded in the HSDP-2 drill core. Geochem Geophys Geosyst 4:8710. https://doi.org/10.1029/2002GC000339

Ellam RM, Hawkesworth CJ, Menzies MA, Rogers NW (1989) The volcanism of southern Italy: role of subduction and the relationships between potassic and sodic alkaline magmatism. J Geophys Res 94:4589–4601

Esperança S, Crisci GM (1995) The island of Pantelleria: a case for the development of DMM-HIMU isotopic compositions in a long-lived extensional setting. Earth Planet Sci Lett 136:167–182

Esperança S, Crisci GM, De Rosa R, Mazzuoli R (1992) The role of the crust in the magmatic evolution of the Island of Lipari (Aeolian Islands, Italy). Contrib Mineral Petrol 112:450–562

Fiannacca P, Williams IS, Cirrincione R, Pezzino A (2008) Crustal contributions to Late Hercynian peraluminous magmatism in the southern Calabria-Peloritani orogen, southern Italy: petrogenic inferences and the Gondwana connection. J Petrol 49:1497–1514

Francalanci L, Taylor SR, McCulloch MT, Woodhead JD (1993) Geochemical and isotopic variations in the calc-alkaline rocks of Aeolian arc, southern Tyrrhenian Sea, Italy: constraints on magma genesis. Contrib Mineral Petrol 113:300–313

Frey F, Prinz M (1978) Ultramafic inclusions from San Carlos, Arizona: Petrologic and geochemical data bearing on their petrogenesis. Earth Planet Sci Lett 38:129–176

Gasperini D, Blichert-Toft J, Bosch D, Del Moro A, Macera P, Albarède F (2002) Upwelling of deep mantle material through a plate window: evidence from the geochemistry of Italian basaltic volcanics. J Geophys Res 107(B12):2367

Gertisser R, Keller J (2000) From basalt to dacite: origin and evolution of the calc alkaline series of Salina, Aeolian Arc, Italy. Contrib Mineral Petrol 139:607–626

Ghiorso MS, Sack RO (1995) Chemical mass-transfer in magmatic processes IV. A revised and internally consistent thermodynamic model for the interpolation and extrapolation of liquid-solid equilibria in magmatic systems at elevated temperatures and pressures. Contrib Mineral Petrol 119(2–3):197–212

Ghiorso M S, Hirschmann MM, Reiners PW, Kress VC III (2002) The pMELTS: a revision of MELTS for improved calculation of phase relations and major element partitioning related to partial melting of the mantle to 3 GPa. Geochem Geophys Geosyst. https://doi.org/10.1029/2001GC000217

Gioncada A, Mazzuoli R, Bisson M, Pareschi MT (2003) Petrology of volcanic products younger than 42 ka on the Lipari-Vulcano complex (Aeolian Islands, Italy): an example of volcanism controlled by tectonics. J Volcanol Geotherm Res 122:191–220

Guest JE, Chester DK, Duncan AM (1984) The Valle del Bove, Mount Etna: its origin and relation to the stratigraphy and structure of the volcano. J Volcanol Geotherm Res 21:1–23

Gvirtzman Z, Nur A (1999) The formation of Mount Etna as the consequence of slab rollback. Nature 401:782–785

Hanan BB, Graham DW (1996) Lead and helium isotope evidence from oceanic basalts for a common deep source of mantle plumes. Science 272:991–995

Hart SR (1984) The DUPAL anomaly: a large-scale isotopic anomaly in the southern hemisphere. Nature 309:753–756

Hart SR, Hauri EH, Oschmann LA, Whitehead JA (1992) Mantle plumes and entrainment: isotopic evidence. Science 256:517–520

Harte B, Hunter RH, Kinny PD (1993) Melt geometry, movement and crystallization in relation to mantle dykes, veins and metasomatism. Philos Trans R Soc Lond Ser A 342:1–21

Hegner E, Walter HJ, Satir M (1995) Pb–Sr–Nd isotopic compositions and trace element geochemistry of megacrysts and melilitites from the Tertiary Urach volcanic field: source composition of small volume melts under SW Germany. Contrib Mineral Petrol 122(3):322–335

Hoernle K, Zhang YS, Graham D (1995) Seismic and geochemical evidence for large-scale mantle upwelling beneath the eastern Atlantic and western and central Europe. Nature 374:339

Irving AJ (1980) Petrology and geochemistry of composite ultramafic xenoliths in alkalic basalts and implications for magmatic processes within the mantle. Am J Sci 280A:389–426

Joron J-L, Treuil M (1989) Hygromagmaphile element distributions in oceanic basalts as fingerprints of partial melting and mantle heterogeneities: a specific approach and proposal of an identification and modelling method. Geol Soc Lond Spec Publ 42(1):277–299. https://doi.org/10.1144/GSL.SP.1989.042.01.17

Kahl M, Chakraborty S, Pompilio M, Costa F (2015) Constraints on the nature and evolution of the magma plumbing system of Mt. Etna volcano (1991–2008) from a combined thermodynamic and kinetic modelling of the compositional record of minerals. J Petrol 56(10):2025–2068. https://doi.org/10.1093/petrology/egv063

Kamenetsky VS, Pompilio M, Métrich N, Sobolev AV, Kuzmin DV, Thomas R (2007) Arrival of extremely volatile-rich high-Mg magmas changes explosivity of Mount Etna. Geology 35:255. https://doi.org/10.1130/G23163A.1

Kempton PD (1987) Mineralogic and geochemical evidence for differing styles of metasomatism in spinel lherzolite xenoliths: enriched mantle source regions of basalts. In: Menzies M, Hawkesworth CJ (eds) Mantle metasomatism. Academic Press, London, pp 45–89

Kempton PD, Downes H, Lustrino M (2018) Pb and Hf isotope evidence for mantle enrichment processes and melt interactions in the lower crust and lithospheric mantle in Miocene orogenic volcanic rocks from Monte Arcuentu (Sardinia, Italy). Geosphere 14:926–950. https://doi.org/10.1130/GES01584.1

Kieffer G, Tanguy J-C (1993) L'Etna: évolution structurale, magmatique et dynamique d'un volcan "polygenique." Mem Soc Geol Fr 163:253–271

Klaver M, Djuly T, de Graaf S, Sakes A, Wijbrans J, Davies G, Vroon P (2015) Temporal and spatial variations in provenance of Eastern Mediterranean Sea sediments: implications for Aegean and Aeolian arc volcanism. Geochim Cosmochim Acta 153:149–168

Kogiso T, Hirschmann MM, Frost DJ (2003) High-pressure partial melting of garnet pyroxenite: possible mafic lithologies in the source of ocean island basalts. Earth Planet Sci Lett 216:603–617

Lambart S, Baker MB, Stolper EM (2016) The role of pyroxenite in basalt genesis: Melt-PX, a melting parameterization for mantle pyroxenites between 0.9 and 5 GPa. J Geophys Res Solid Earth 121:5708–5735. https://doi.org/10.1002/2015JB012762

Le Maitre RW (1984) A proposal by the IUGS Subcommission on the Systematics of Igneous Rocks for a chemical classification of volcanic rocks based on the total alkali silica (TAS) diagram. Aust J Earth Sci 31:243–255

Lo Giudice A (1970) Caratteri petrografici e petrochimici delle lave del Complesso di Vavalaci (Etna). Rend Soc Ital Mineral Et Petrol 26:687–732

Marty B, Trull T, Lussiez P, Basile I, Tanguy J-C (1994) He, Ar, O, Sr and Nd isotope constraints on the origin and evolution of Mount Etna magmatism. Earth Planet Sci Lett 126:23–39

McGuire WJ (1982) Evolution of the Etna volcano: information from the southern wall of the Valle del Bove caldera. J Volcanol Geotherm Res 13:241–271

Michaud V (1995) Crustal xenoliths in recent hawaiites from Mount Etna, Italy: evidence for alkali exchanges during magma-wall rock interaction. Chem Geol 122:21–42

Miller SA, Myers M, Fahnestock MF, Bryce JG, Blichert-Toft J (2017) Magma dynamics of ancient Mt. Etna inferred from clinopyroxene isotopic and trace element systematics. Geochem Persp Lett 4:47–52

Mollo S, Giacomoni PP, Coltorti M, Ferlito C, Iezzia G, Scarlato P (2015) Reconstruction of magmatic variables governing recent Etnean eruptions: Constraints from mineral chemistry and P-T–fO2–H2O modeling. Lithos 212–215:311–320

Nicotra E, Viccaro M, Cristofolini R, Conticelli S (2013) Changes of magma geochemistry at Mt. Etna during the last 45ka due to sampling of a variegated mantle. Goldschmidt Conf Abstr:1846

Orsi G, Civetta L, D'Antonio M, Di Girolamo P, Piochi M (1995) Step-filling and development of a three-layer magma chamber: the Neapolitan Yellow Tuff case history. J Volcanol Geotherm Res 67:291–312

Paonita A, Caracausi A, Iacono-Marziano G, Martelli M, Rizzo A (2012) Geochemical evidence for mixing between fluids exsolved at different depths in the magmatic system of Mt Etna (Italy). Geochim Cosmochim Acta 84:380–394

Pappalardo L, Piochi M, D'Antonio M, Civetta L, Petrini R (2002) Evidence for multi-stage magmatic evolution during the past 60 kyr at Campi Flegrei (Italy) deduced from Sr, Nd and Pb isotope data. J Petrol 43:1415–1434

Patanè G, La Delfa S, Tanguy J-C (2006) Volcanism and mantle-crust evolution: the Etna case. Earth Planet Sci Lett 241:831–843

Patchett PJ, White WM, Feldmann H, Kielinczuk S, Hofmann AW (1984) Hafnium/rare-earth element fractionation in the sedimentary system and crustal recycling into the Earth's mantle. Earth Planet Sci Lett 69:365–378

Peccerillo A (1992) Potassic and ultrapotassic magmatism: compositional characteristics, genesis and geologic significance. Episodes 15:243–251

Peccerillo A, Taylor SR (1976) Geochemistry of Eocene calc-alkaline volcanic rocks from the Kastamonu area, Northern Turkey. Contrib Miner Petrol 58:63–81. https://doi.org/10.1007/BF00384745

Perini G, Francalanci L, Davidson JP, Conticelli S (2004) The petrogenesis of Vico Volcano, Central Italy: an example of low scale mantle heterogeneity. J Petrol 45:139–182

Pilet S, Baker MB, Muentener O, Stolper EM (2011) Monte Carlo simulations of metasomatic enrichment in the lithosphere and implications for the source of alkaline basalts. J Petrol 52:1415–1442

Pinarelli L (1991) Geochemical and isotopic (Sr, Pb) evidence of crust-mantle interaction in silicic melts. The Tolfa-Cerveteri-Manziana volcanic complex (Central Italy): a case history. Chem Geol 92:177–195

Plank T, Langmuir CH (1998) The chemical composition of subducting sediment and its consequences for the crust and mantle. Chem Geol 145:325–394

Prelević D, Stracke A, Foley SF, Romer RL, Conticelli S (2010) Hf isotope compositions of Mediterranean lamproites: mixing of melts from asthenosphere and crustally contaminated mantle lithosphere. Lithos 119:297–312

Prosperini N (1993) Petrologia e geochimica delle rocce dell'isola di Capraia (Arcipelago Toscano, Italia): un vulcano calcalcalino di origine complessa. B.Sc. Thesis, University of Perugia, Italy

Rottura A, Del Moro A, Pinarelli L, Petrini R, Caggianelli PA, A, Bargossi GM, Piccarreta G, (1991) Relationships between intermediate and acidic rocks in orogenic granitoid suites: petrological, geochemical and isotopic (Sr, Nd, Pb) data from Capo Vaticano (southern Calabria, Italy). Chem Geol 92:153–176

Rudnick RL, Gao S (2003) Composition of the continental crust. Treat Geochem 3:1–64

Santo AP, Jacobsen SB, Baker J (2004) Evolution and genesis of calc-alkaline magmas at Filicudi volcano, Aeolian Arc (Southern Tyrrhenian Sea, Italy). Lithos 72:73–96

Scarth A, Tanguy J-C (2001) Volcanoes of Europe. Terra Publishing, pp 51–69

Schiano P, Clocchiatti R, Ottolini L, Busà T (2001) Transition of Mount Etna lavas from a mantle-plume to an islaNd–arc magmatic source. Nature 412:900–904

Scribano V, Viccaro M, Cristofolini R, Ottolini L (2009) Metasomatic events recorded in ultramafic xenoliths from the Hyblean area (Southeastern Sicily, Italy). Mineral Petrol 95:235–250

Smith PM, Asimow PD (2005) Adiabat_1ph: A new public front-end to the MELTS, pMELTS, and pHMELTS models. Geochem Geophys Geosyst. https://doi.org/10.1029/2004GC000816

Spence A, Downes H (2011) A chemostratigraphic investigation of the prehistoric Vavalaci lava sequence on Mount Etna: simulating borehole drilling. Lithos 125:423–433

Spilliaert N, Allard P, Métrich N, Sobolev AV (2006) Melt inclusion record of the conditions of ascent, degassing, and extrusion of volatile-rich alkali basalt during the powerful 2002 flank eruption of Mount Etna (Italy). J Geophys Res 111:B04203

Stracke A, Hofmann AW, Hart SR (2005) FOZO, HIMU and the rest of the mantle zoo. Geochem Geophys Geosyst 6:1–20

Sun SS, McDonough WF (1989) Chemical and isotopic systematics of oceanic basalts: implications for mantle composition and processes. In: Saunders AD, Norry MJ (eds) Magmatism in the ocean basins, vol 42. Geol Soc London Spec Publ., pp 313–345

Tanguy J-C, Condomines M, Kieffer G (1997) Evolution of the Mount Etna magma: constraints on the present feeding system and eruptive mechanism. J Volc Geotherm Res 75:221–250

Thirlwall MF (1991) Long-term reproducibility of multicollector Sr and Nd isotope ratio analysis. Chem Geol Isot Geosci Sect 94:85–104

Thirlwall MF, Jenkins C, Vroon PZ, Mattey DP (1997) Crustal interaction during construction of ocean islands: Pb–Sr–Nd–O isotope geochemistry of the shield basalts of Gran Canaria, Canary Islands. Chem Geol 135(3–4):233–262

Tonarini S, Armienti P, D'Orazio M, Innocenti F, Pompilio M, Petrini R (1995) Geochemical and isotopic monitoring of Mt. Etna 1989–1993 eruptive activity: bearing on the shallow feeding system. J Volcanol Geotherm Res 64:95–115

Tonarini S, D'Orazio M, Armienti P, Innocenti F, Scribano V (1996) Geochemical features of eastern Sicily lithosphere as probed by Hyblean xenoliths and lavas. Eur J Miner 8:1153–1173

Tonarini S, Armienti P, D'Orazio M, Innocenti F (2001) Subduction-like fluids in the genesis of Mt. Etna magmas: evidence from

boron isotopes and fluid mobile elements. Earth Planet Sci Lett 192:471–483

Trua T, Esperança S, Mazzuoli R (1998) The evolution of the lithospheric mantle along the N. African Plate: geochemical and isotopic evidence from the tholeiitic and alkaline volcanic rocks of the Hyblean Plateau, Italy. Contrib Miner Petrol 131:307–322

Vervoort JD, Blichert-Toft J, Patchett PJ, Albarède F (1999) Relationships between Lu–Hf and Sm–Nd isotopic systems in the global sedimentary system. Earth Planet Sci Lett 168:79–99

Vervoort JD, Patchett PJ, Albarède F, Blichert-Toft J, Rudnick R, Downes H (2000) Hf-Nd isotopic evolution of the lower crust. Earth Planet Sci Lett 181:115–129

Viccaro M, Cristofolini R (2008) Nature of mantle heterogeneity and its role in the short-term geochemical and volcanological evolution of Mt. Etna (Italy). Lithos 105:272–288

Viccaro M, Zuccarello F (2017) Mantle ingredients for making the fingerprint of Etna alkaline magmas: implications for shallow partial melting within the complex geodynamic framework of Eastern Sicily. J Geodyn 109:10–23

Viccaro M, Nicotra E, Millar IL, Cristofolini R (2011) The magma source at Mount Etna volcano: Perspectives from the Hf isotope composition of historic and recent lavas. Chem Geol 281:343–351

Vollmer R (1976) Rb-Sr and U-Th-Pb systematics of alkaline rocks: the alkaline rocks from Italy. Geochim Cosmochim Acta 40:283–295

White WM, Patchett PJ, Ben Othman D (1986) Hf isotope ratios of marine sediments and Mn nodules: evidence for a mantle source of Hf in seawater. Earth Planet Sci Lett 79:46–54

White WM, Albarède F, Télouk P (2000) High-precision analysis of Pb isotope ratios by multi-collector ICP-MS. Chem Geol 167:257–270

Willbold M, Stracke A (2006) Trace element composition of mantle eNd–members: Implications for recycling of oceanic and upper and lower continental crust. Geochem Geophys Geosyst 7(4):Q04004. https://doi.org/10.1029/2005GC001005

Wilson M, Downes H (2006) Tertiary-Quaternary intra-plate magmatism in Europe and its relationship to mantle dynamics. Eur Lithosphere Dyn Geol Soc Lond Mem 32:147–166

Wilson M, Downes H, Cebriá J-M (1995) contrasting fractionation trends in coexisting continental alkaline magma series; Cantal, Massif Central, France. J Petrol 36(6):1729–1753. https://doi.org/10.1093/oxfordjournals.petrology.a037272